Electronic Supplementary Material (ESI) for Journal of Materials Chemistry B.

Self-assembled vesicle and rod-like aggregates of functionalized perylene diimide: Reaction based near-IR intracellular fluorescent probe for selective detection of palladium

Prabhpreet Singh,*[a] Lalit Singh Mittal,[a] Vanita Vanita,[b] Kapil Kumar,[a] Amandeep Walia,[b] Gaurav Bhargava,[c] Subodh Kumar[a]

[a] Dr. P. Singh, L.S. Mittal, K. Kumar, Prof. Dr. S. Kumar
Department of Chemistry, UGC Centre for Advanced Studies, Guru Nanak Dev University, Amritsar 143 005, India
[b] Prof. Dr. V. Vanita, A. Walia
Department of Human Genetics, Guru Nanak Dev University, Amritsar 143 005, India
[c] Dr. G. Bhargava
Department of Applied Sciences, Punjab Technical University, Kapurthala 144601, Punjab, India

Table: Comparison of solvent, detection limits and applications in live cell imaging and environmental samples of present work with literature report.

Published	Solvent	Metal	Detection limit	Cell study	Practical Application
Present Work	**THF:H_2O (1:1)** **DMSO:H_2O (1:9)**	**Pd^0, Pd^{2+}**	**THF:H_2O (1:9) 120 nM** **DMSO:H_2O (1:9) 6.6 nM**	**HeLa Cell**	**Pd^0 analysis in pharmaceutical, environmental and urine samples.**
Analyst **2016**, DOI: 10.1039/C6AN00204H	PBS solution	Pd^0	2.1 nM	HeLa Cells	No
Tetrahedron letter, 2016, 57, 1451-1455	DMSO:H_2O (1:1)	Pd^0	0.34 nM	No	No
Chem. Asian Journal 2016, 11, 43-48	EtOH:H_2O (1:1)	Pd^0, Pd^{2+}	191 nM	Zebra fish, Dapnia magna	No
Tetrahedron Letter, 2015, 56, 6491-6494	DMSO:H_2O(9:1)	Pd^0	52 nM	No	No
Tetrahedron 2015, 71, 7874-7878	DMSO:H_2O(1:1)	Pd^0	17.4 nM	No	No
Tetrahedron Letter, 2014, 55, 2537-2540	DMSO:H_2O (8:2)	Pd^0, Pd^{2+}	12 nM Pd^{+2}	No	Water and fetal bovine serum.
Inorganic Chem. 2014, 53, 12590-12594	PBS solution (1% organic solvent)	Pd^0, Pd^{2+}	25 nM Pd^{+2}	Yes	No
Anal. Chim. Acta, 2013, 786, 139-145.	CTAB micellar solution	Pd^0	1 μM	No	Pd in chemical reactions and catalytic converters.
Analyst 2013, 138, 1564	CH_3CN : H_2O (1:1)	Pd^0, Pd^{2+}	-	No	No
Chem. Commun., 2012, 48, 2867-2869	CH_3CN : H_2O (1:4)	Pd^0, Pd^{2+}, Pd^{4+}	87 nM	No	Biological and environmental
Sensor Actuat B., 2012, 171-172, 1277-1282	CH_3OH : PBS (8:2)	Pd^0, Pd^{2+}, Pd^{4+}	0.05 μM Pd^{+2}	No	Environmental

Chem. Commun., 2011, 47, 8656-8658	PBS	Pd^0, Pd^{2+}, Pd^{4+}	0.07 μM	Yes	No
Organic Letter 2011, 13, 4922-4925	CH_3CN : H_2O (4:1)	Pd^0, Pd^{2+}, Pd^{4+}	6.1 nM Pd^{+2}	No	Environmental samples
Chem. Commun., 2010, 46, 3964-3966	CH_3CN: H_2O (1:9)	Pd^0, Pd^{2+}, Pd^{4+}	191 nM	Zebra Fish imaging	No
Chem. Commun., 2009, 86-88	DMSO:H_2O (1:1)	Pd^0	10 nM	No	Soil.
JACS 2007, 129, 12354-12355	Borate Buffer	Pd^0, Pd^{2+}	3 nM	No	Pharmaceutical, mining industry

2. Experimental Section

Cell Imaging and MTT assay studies

Cell imaging studies were performed using HeLa cell line. HeLa cells were grown in Dulbecco's modified Eagle's medium (DMEM) that was supplemented with 10% fetal bovine serum (FBS), 100 IU/ml penicillin, 100 μg/ml streptomycin and 100 μg/ml gentamycin. HeLa cells were grown and maintained in a humidified environment in an incubator at 37 ^oC with 5% CO_2. A day before treatment, a total of $2x10^5$ cells were seeded on glass coverslips (11 mm size) into the wells of a 24-well plate, and HeLa cells were grown for 24 hours (until 65-70% confluence). Treatment was carried out in triplicates in FBS and antibiotics free DMEM (90%) with DMSO (10%). HeLa cells were incubated with **PS-PDI** (10 μM) at 37 ^oC with 5% CO_2 for 30 min. followed by 2 times wash with 1X phosphate buffered saline (PBS) (pH = 7.4) supplemented with 10% DMSO and the addition of Pd^0 (20 and 40 μM) for four hours by incubating the cells at identical conditions. The HeLa cells were then washed thrice with 1X PBS supplemented with 10% DMSO, fixed in 4% paraformaldehyde (ice cold), again washed three times with 1X PBS supplemented with 10% DMSO and mounted on to the glass slides. To test the cytotoxicity of **PS-PDI**, MTT [3-(4,5-dimethylthiazol- 2-yl)-2,5-diphenyltetrazolium bromide] assay was performed with HeLa cells so as to determine the effect of **PS-PDI** on proliferation of cells. The fluorescent signals were visible in the cytoplasmic region of the HeLa cells sparing the nuclei. Brightfield imaging after treatment with **PS-PDI** and Pd^0 indicated that cells were viable throughout the experiment. HeLa cells were observed to be permeable to both the **PS-PDI** and Pd^0**.**

Preparation of samples and photophysical studies

Method for Detection of Pd^{2+}: **PS-PDI** was added in various 10 mL volumetric flask and subsequently different concentrations of $PdCl_2$ as a source of Pd^{2+} were added followed by addition of 350 μL of 10 mM solution of $NaBH_4$ and 350 μL of 10 mM solution of PPh_3. The solutions were diluted with HEPES buffer-THF (1:1 v/v, pH 7.3) up to the 10 mL mark. Then solutions were kept for 1h for equilibration before taking the readings. *Preparation of drug samples*: For performing the UV-Vis titration of **PS-PDI** in drug samples, the following procedure was followed. To the 10 μM solution of **PS-PDI** in HEPES buffered THF (1:1 v/v, pH 7.3), we dissolved 1 or 5 mg drug (Disprin tablet, which contain 0.64 or 3.5 mg of Aspirin, respectively) followed by addition of various concentration of Pd^0 in different volumetric flasks. The volume of the solution in each flask was finally adjusted to 10 mL and prepared solutions were kept for 1h before taking the final reading. Similarly, the same protocol was followed to prepare different solution containing Pd^{2+} + $NaBH_4$-PPh_3 as a reducing agent in Disprin drug. Furthermore, a similar new set of solutions of **PS-PDI** were also prepared with Pd^0 and Pd^{2+} with $NaBH_4$-PPh_3 without the addition of Disprin tablet and flasks were equilibrated for 1h before taking the final reading. *Preparation of environmental samples*: The measurements of optical properties of **PS-PDI** towards Pd^0 were also performed in the environmental samples such as tap water, pond water and industrial waste water. For preparing the solution of **PS-PDI** (10 μM) in these environmental samples, the de-ionized water in THF:water (1:1 v/v, pH 7.3) was replaced by tap water, or pond water or industrial waste water as per design of the experiment followed by addition of various concentration of Pd^0. The samples were equilibrated for 1h and then UV-Vis and fluorescence spectra were recorded. *UV-Visible and Fluorescence titrations:* The stock solutions for various measurements of **PS-PDI, DPS-PDI, PDI 5** and **PDI-OH** were prepared and dilutions of these stock solutions were used for the photophysical measurements. We have used $Pd(PPh_3)_4$ as a source of Pd^0 whereas $PdCl_2$ was used as source of Pd^{2+} ions. Other metal ions were used as their perchlorate or nitrate salts. All absorption and fluorescence scans were saved as ACSII files and further processed in Excel™ to produce all graphs shown in the manuscript. *DLS measurements*: The solutions were filtered with a Millipore membrane filter (Acrodisc syringe filter, 0.45 μm Supor membrane) before measurements. The samples were thermally equilibrated for 10 min before each measurement, and an average of 10 measurement runs were considered to be data. *SEM/TEM images*: Samples of PDI **1** were dissolved in DMSO:H_2O (1:9 v/v). 5 μL aliquot of fresh solution of PDI **1** was deposited on glass surface using drop cast method. After drying the glass surface was imaged.

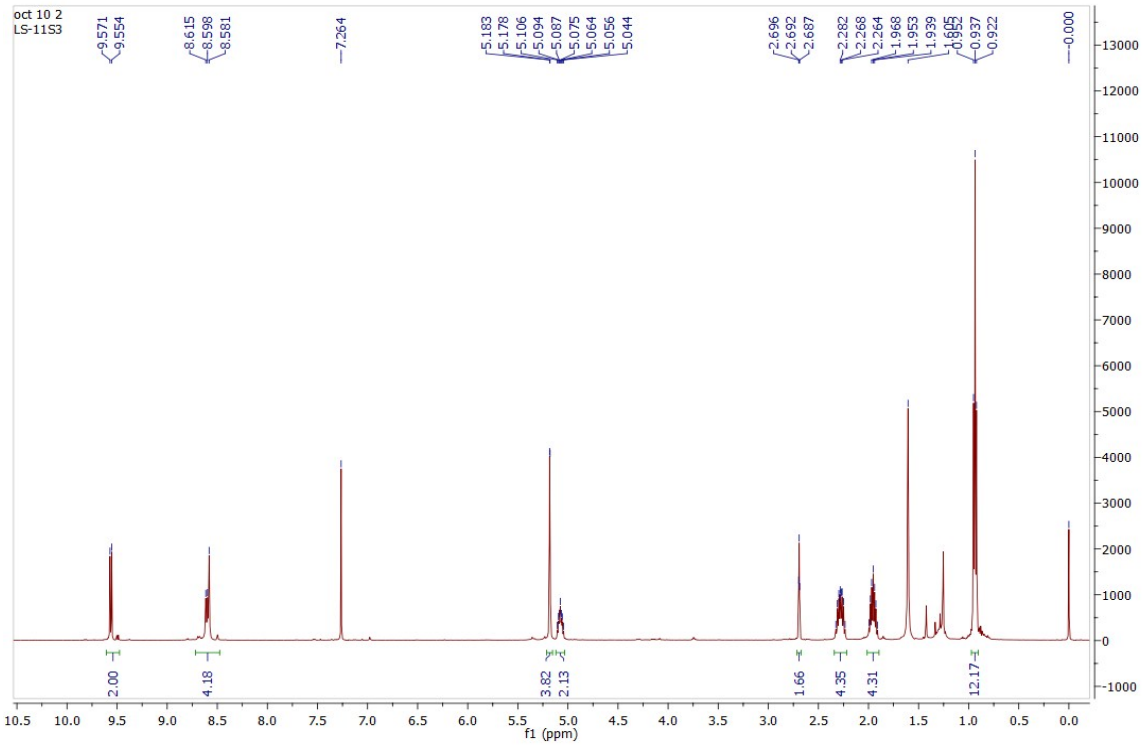

Fig S1a: [1]H NMR spectrum of **DPS-PDI**.

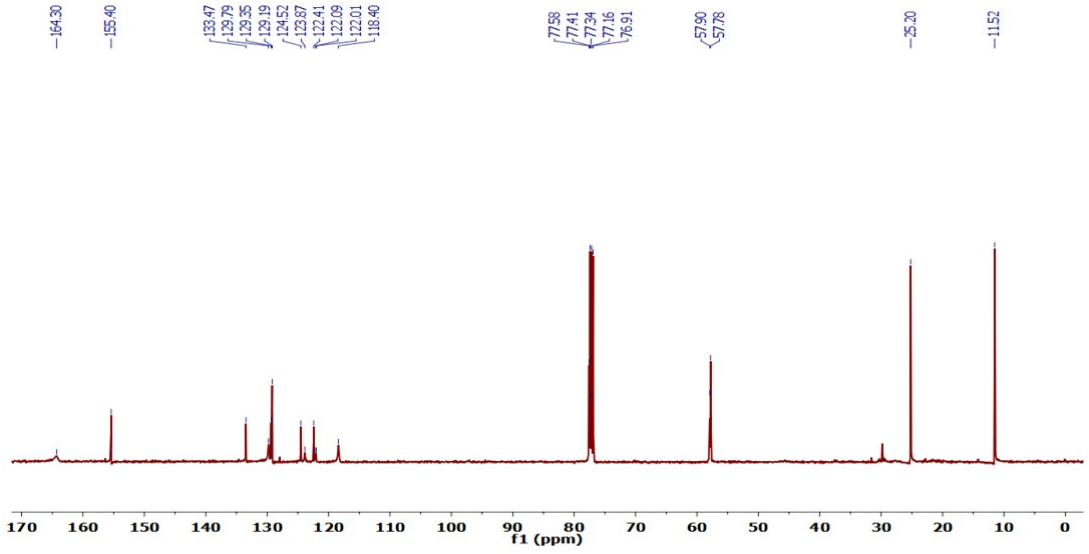

Fig S1b: [13]C NMR spectrum of **DPS-PDI**.

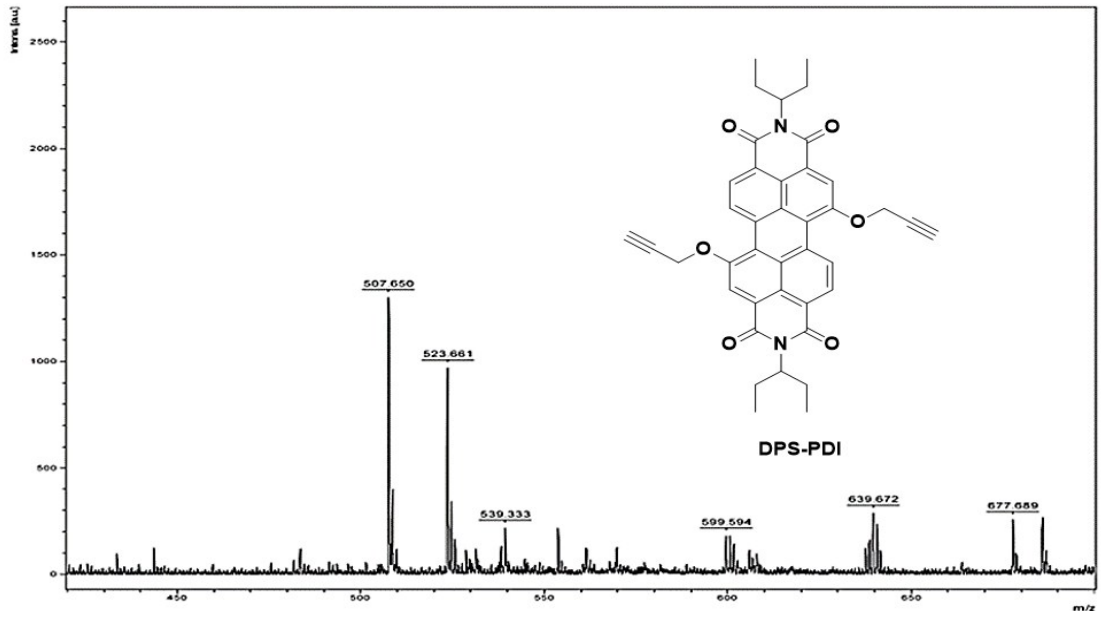

Fig S1c: Mass spectrum of **DPS-PDI**.

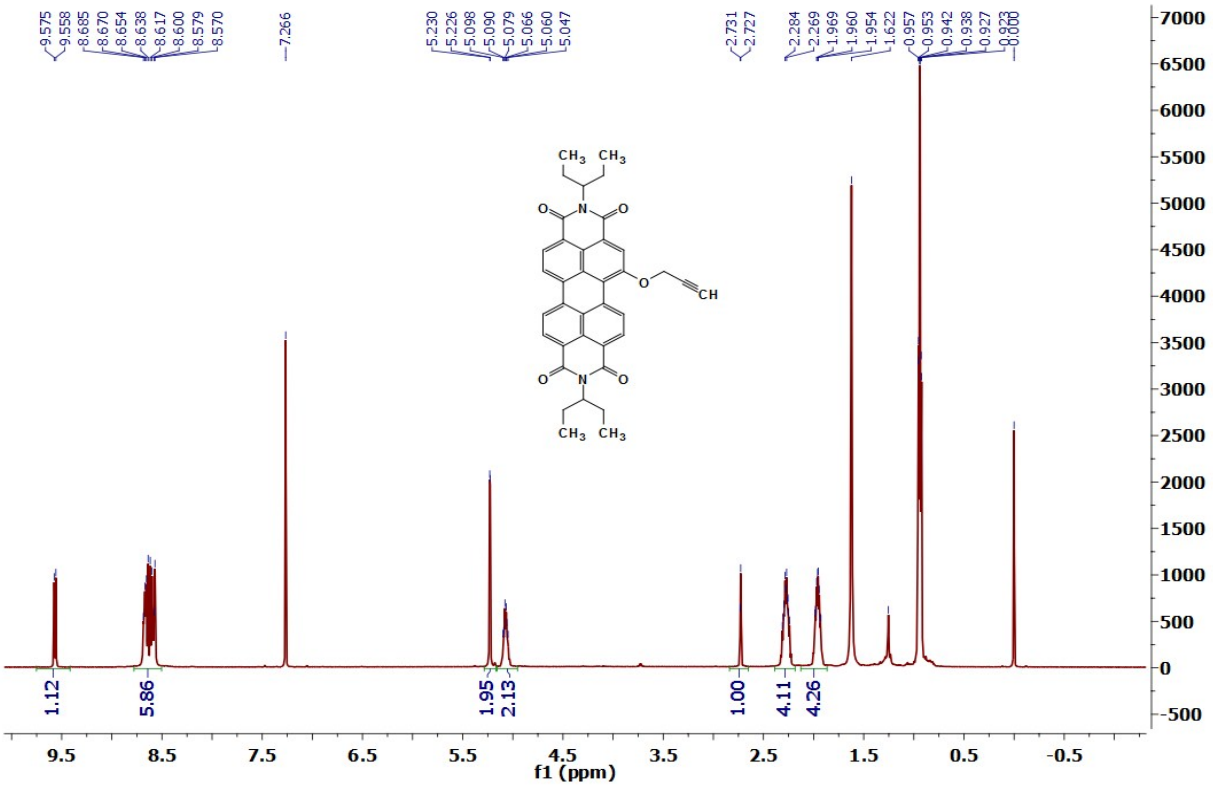

Fig S2a: [1]H NMR spectrum of **PS-PDI**

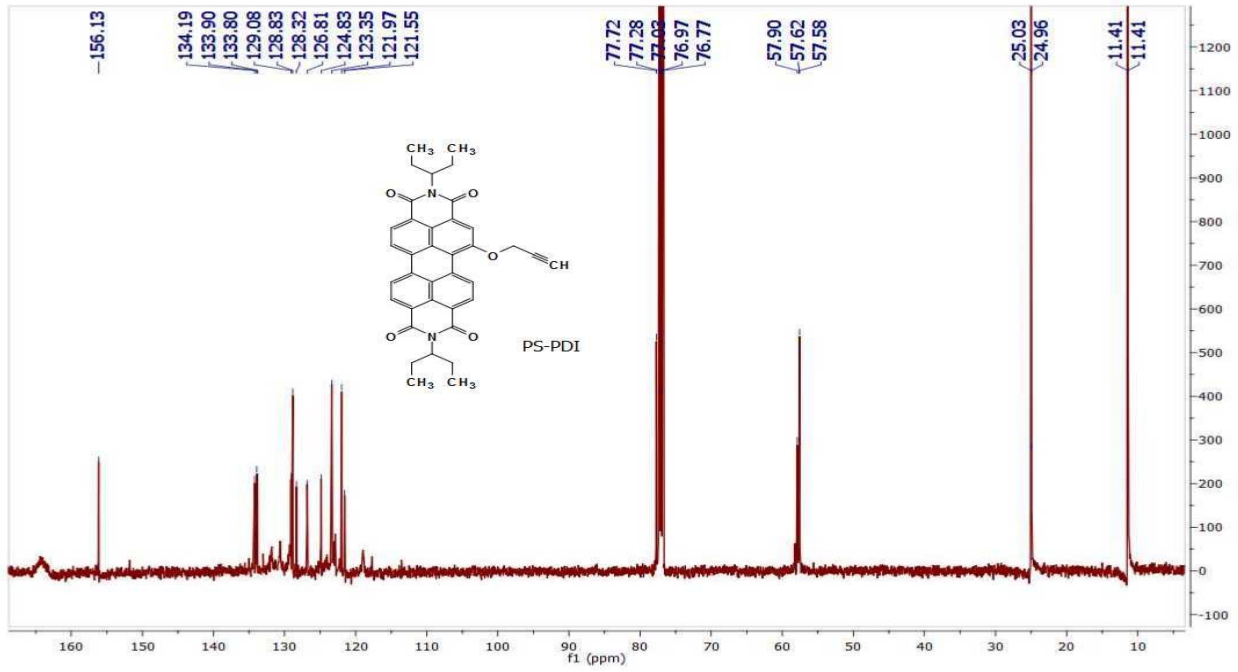

Fig S2b: ^{13}C NMR spectrum of **PS-PDI**.

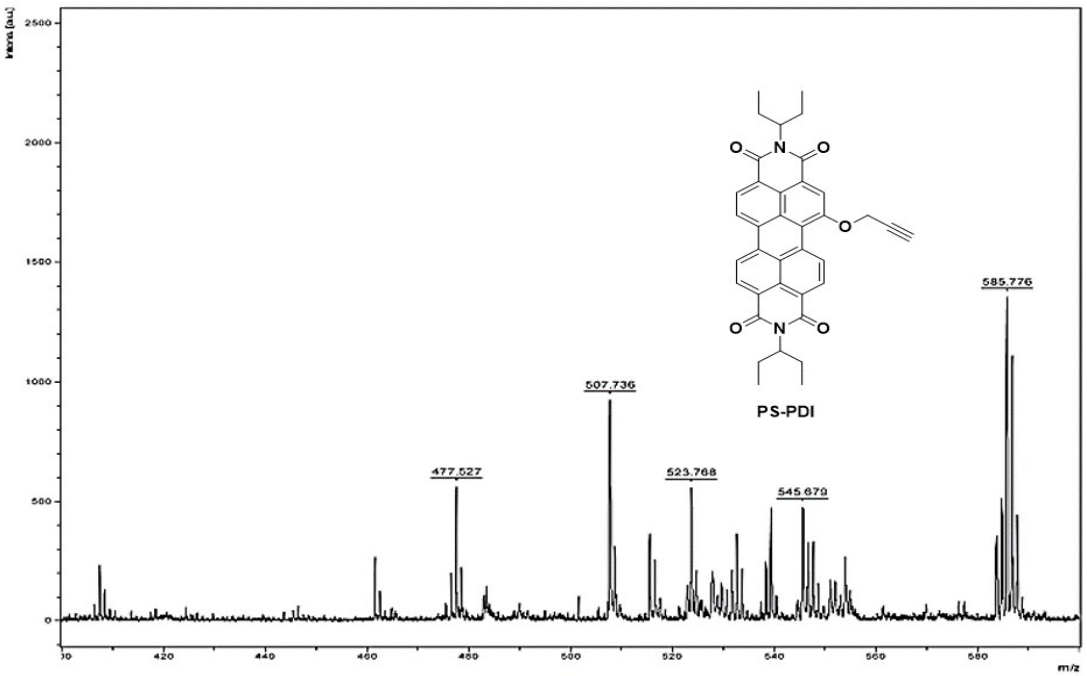

Fig S2c: Mass spectrum of **PS-PDI.**

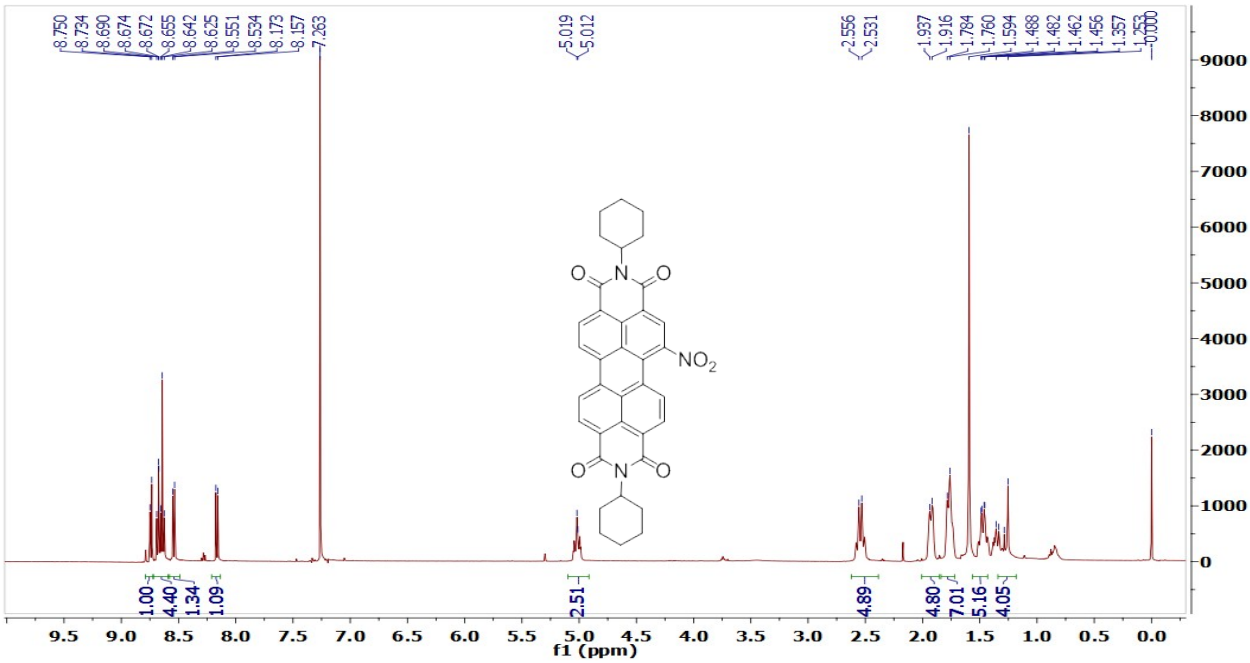

Fig S3a: [1]H NMR spectrum of PDI **4**.

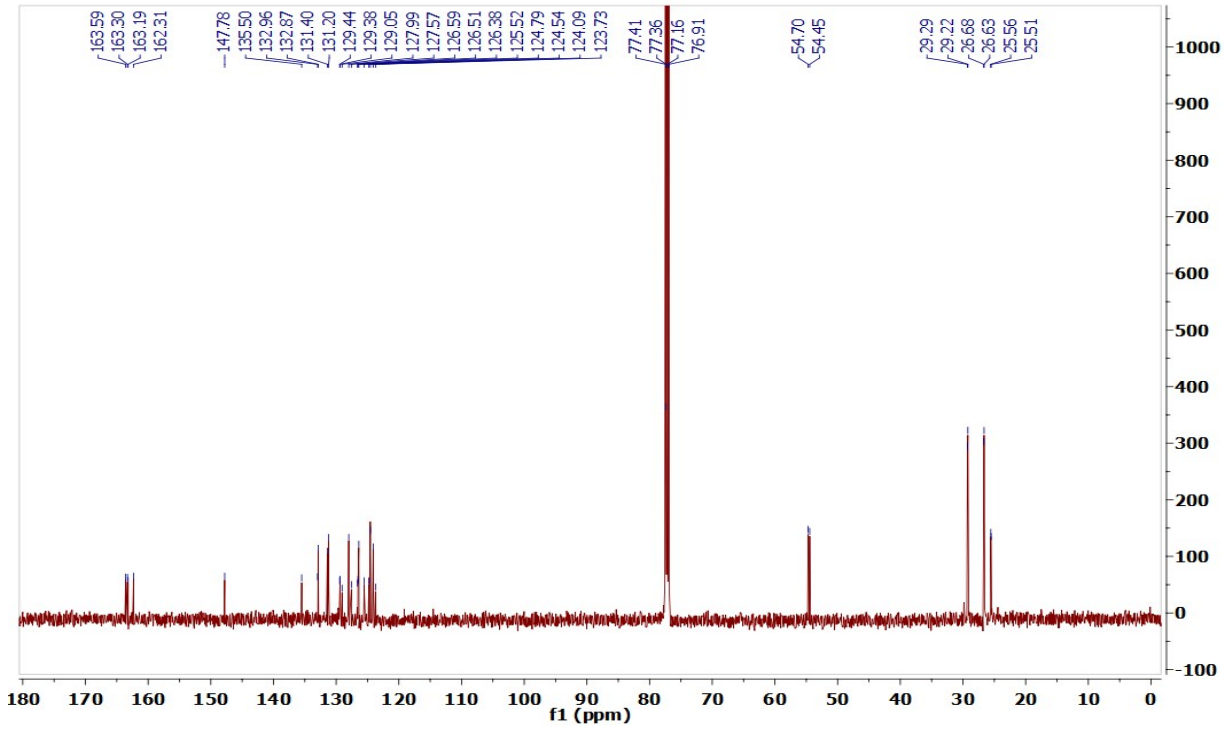

Fig S3b: [13]C NMR spectrum of PDI **4**.

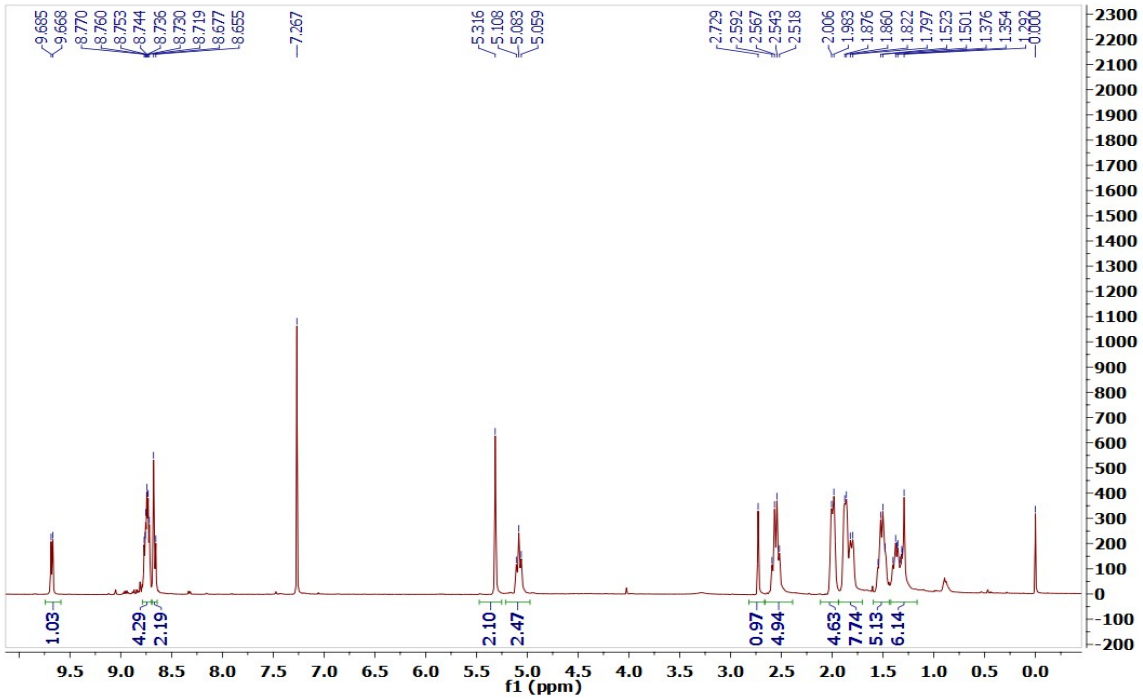

Fig S4a: [1]H NMR spectrum of PDI **5**.

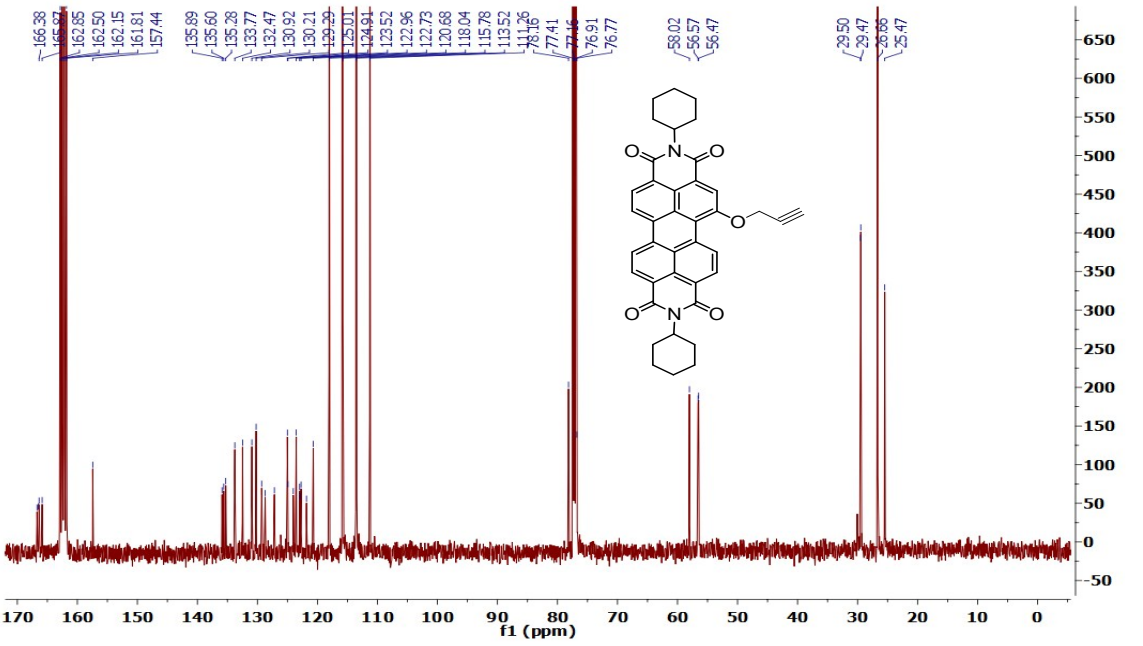

Fig S4b: [13]C NMR spectrum of PDI **5**.

3. Photophysical properties of PS-PDI in different Solvents

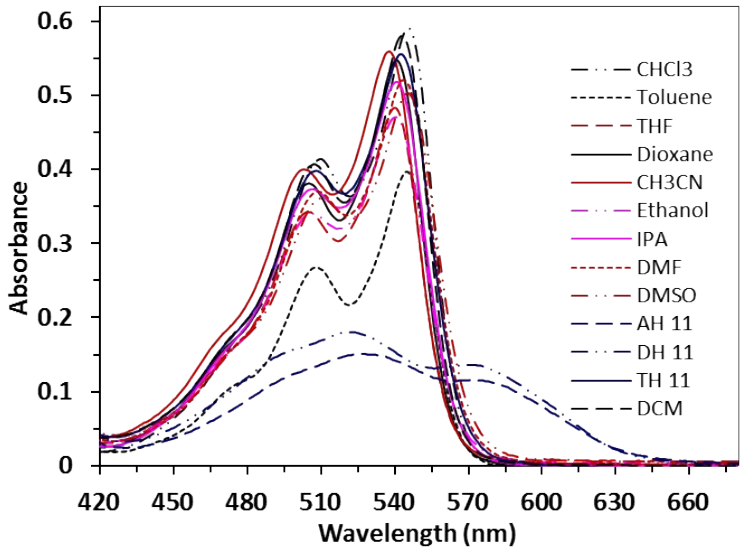

Fig. S5a. Solvent dependent absorption spectrum of **PS-PDI** (10 μM) recorded in different polarity solvents. A:H = Acetonitrile:H_2O; D:H = DMSO:H_2O; T:H = THF:H_2O.

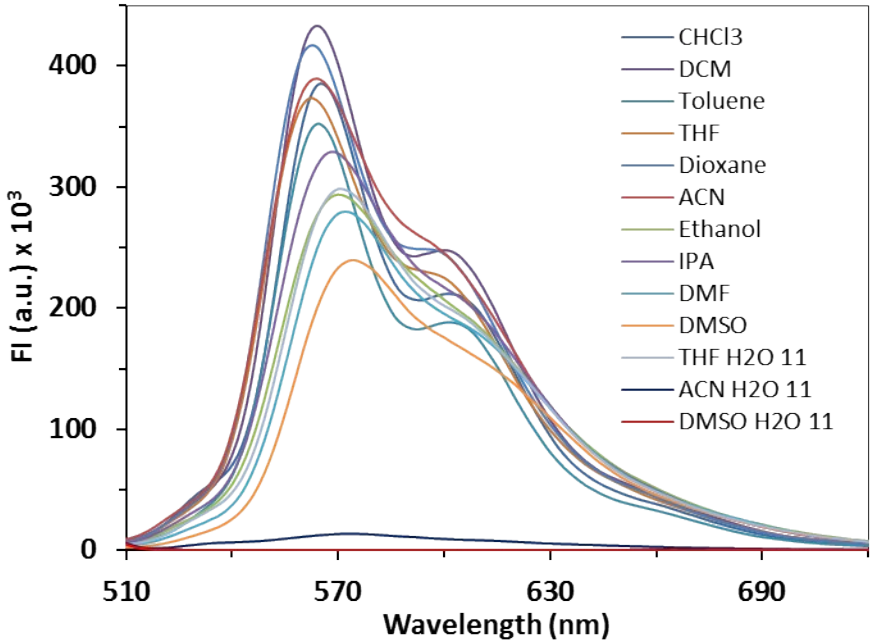

Fig. S5b. Solvent dependent fluorescence spectrum of **PS-PDI** (10 μM) recorded in different polarity solvents; λ_{ex}490 nm; slit width (Ex/Em = 10/10 nm).

Table S1: Spectroscopic and photophysical characteristics of **PS-PDI** in various solvents.

Solvents	**λ_{abs} (nm) (ε)**	**λ_{em} (nm) (FI)**	**ν_{abs}[a]x10^4 (cm^{-1})**	**ν_{flu}[b]x10^4 (cm^{-1})**	**A_{0-0}/A_{0-1} ratio[c]**	**(ν_A-ν_F)[d] (cm^{-1})**	**Quantum Yield[e] Φ**
$CHCl_3$	545 (59000)	564 (387568)	1.834	1.773	1.42	610	0.840
Toluene	545 (39700)	564 (355936)	1.834	1.773	1.47	610	0.900
THF	540 (48300)	562 (373969)	1.851	1.779	1.40	720	0.743
Dioxane	541 (54700)	564 (419172)	1.848	1.773	1.43	750	0.744
CH_3CN	538 (55900)	564 (392211)	1.858	1.754	1.41	850	0.627
Ethanol	540 (47000)	570 (295260)	1.851	1.754	1.38	970	0.640
IPA	541 (51800)	570 (329939)	1.848	1.754	1.33	940	0.645
DMSO	545 (50200)	574 (240822)	1.834	1.742	1.39	920	0.630
DCM	543 (58000)	564 (435251)	1.841	1.773	1.42	680	0.720
H_2O	513 (14900)	Weak Fluorescence	1.94	-----	0.61	-----	-----
TH 1:1	544 (55100)	572 (297060)	1.838	1.748	1.40	900	-----
AH 1:1	529 (15000)	574 (13187)	1.890	1.742	0.76	1480	-----
DH 1:1	522 (18000)	Weak Fluorescence	1.915	-----	0.75	-----	-----

[a]Maximum absorption wavenumbers, [b]Maximum fluorescent wavenumbers, [c]Lippert-Mataga polarity parameter(Δf) [1], [d]Stoke's shift, [e]Fluorescence quantum yield. The fluorescence quantum yields (φ_f) were determined using rhodamine B [2] as a reference with the known $\varphi_f = 0.5$ in ethanol; slit width (excitation = 1 nm, emission = 1 nm).

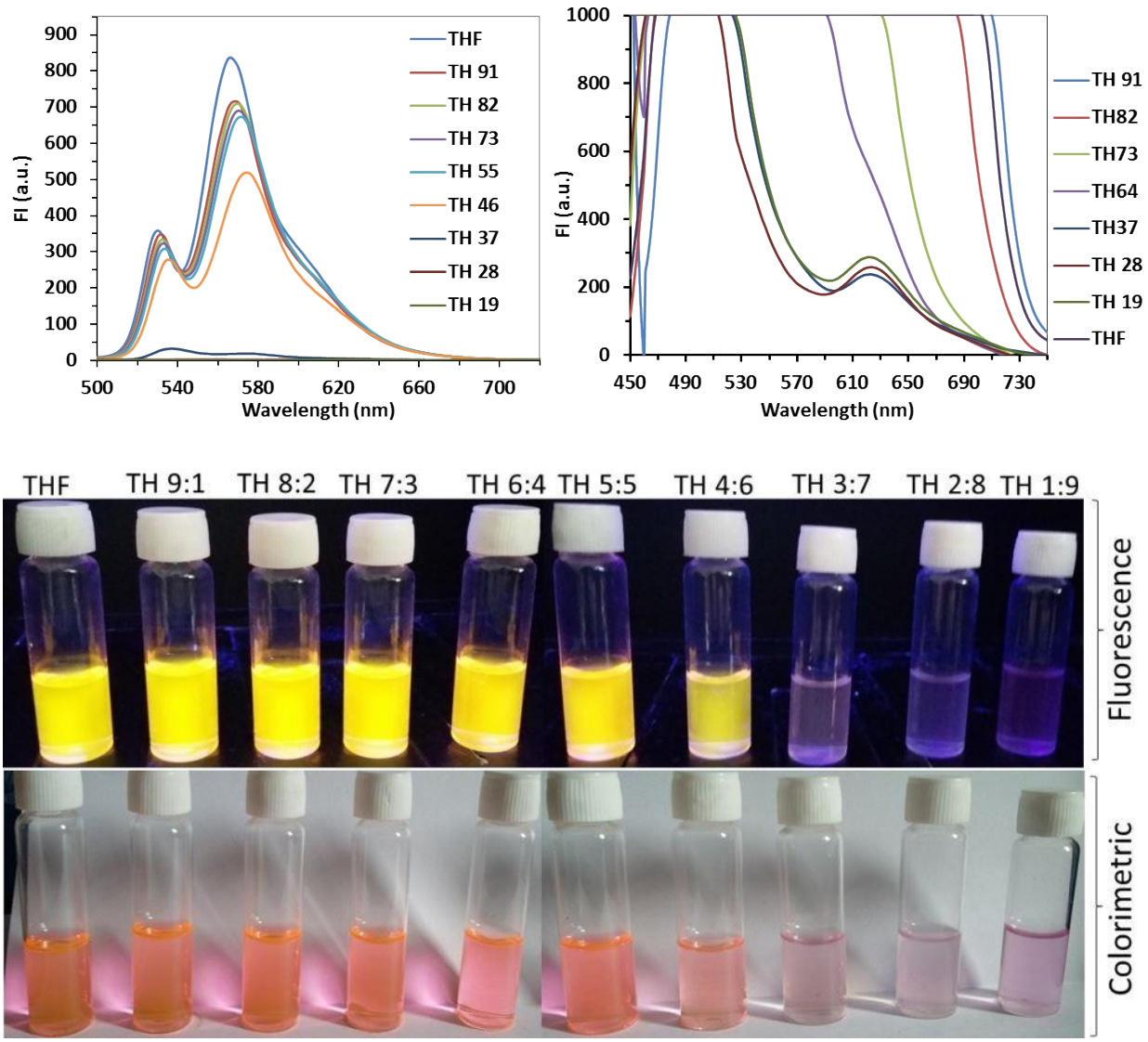

Fig. S6a. (Upper panel) Fluorescence spectra of **PS-PDI** (10 μM) after incremental addition of water in THF (Left, with λ_{ex} 470 nm, slit width Ex/Em = 15/2.5) and (Right, with λ_{ex} 490 nm, slit width Ex/Em = 20/20); (Lower panel) Fluorescence and Sunlight photographs of **PS-PDI** (10 μM) after incremental addition of water in THF.

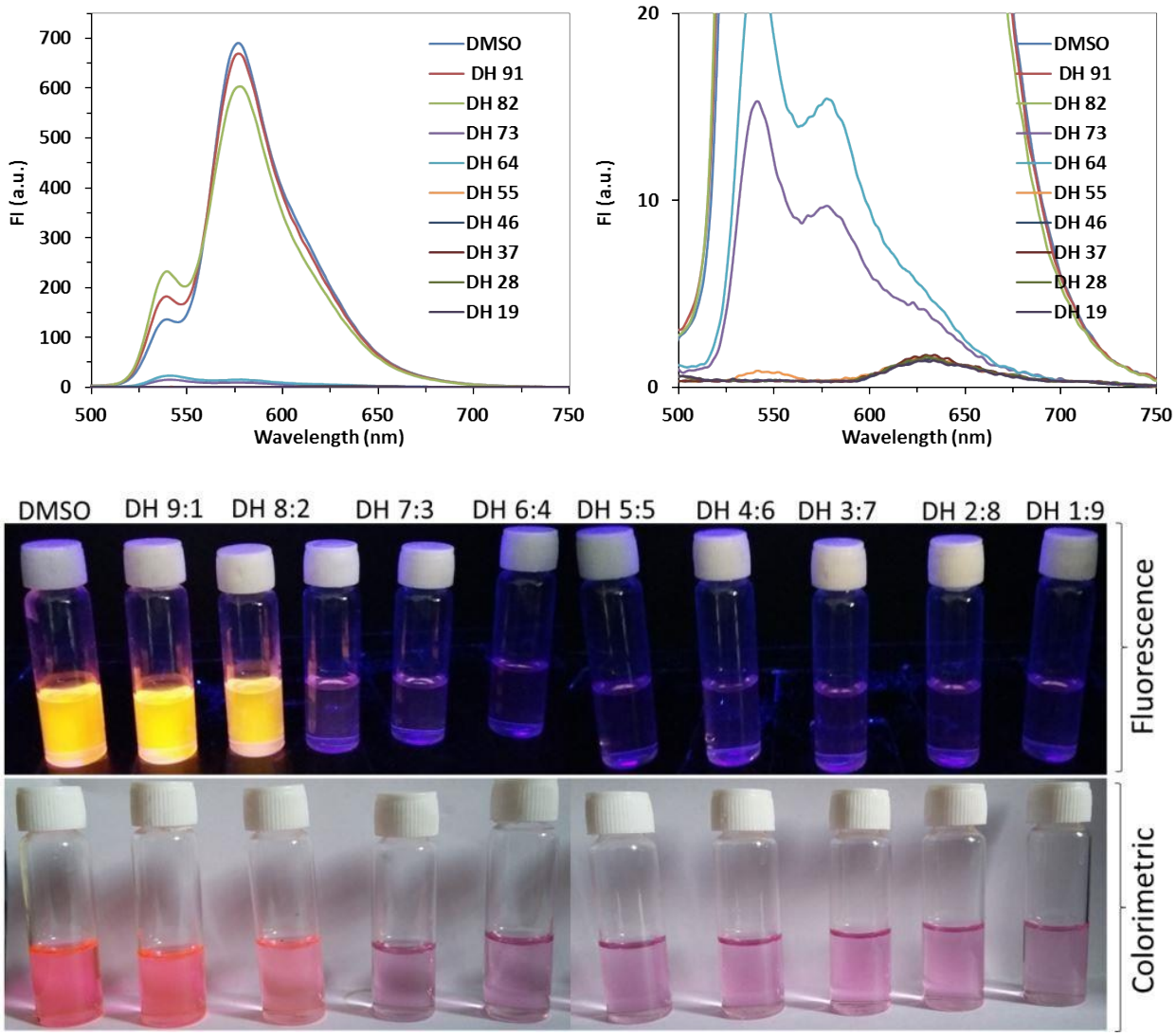

Fig. S6b. (Upper panel) Fluorescence spectra of **PS-PDI** (10 μM) after incremental addition of water in DMSO (Left, with λ_{ex} 470 nm, slit width Ex/Em = 15/3.5) and (Right, expansion); (Lower panel) Fluorescence and Sunlight photographs of **PS-PDI** (10 μM) after incremental addition of water in DMSO.

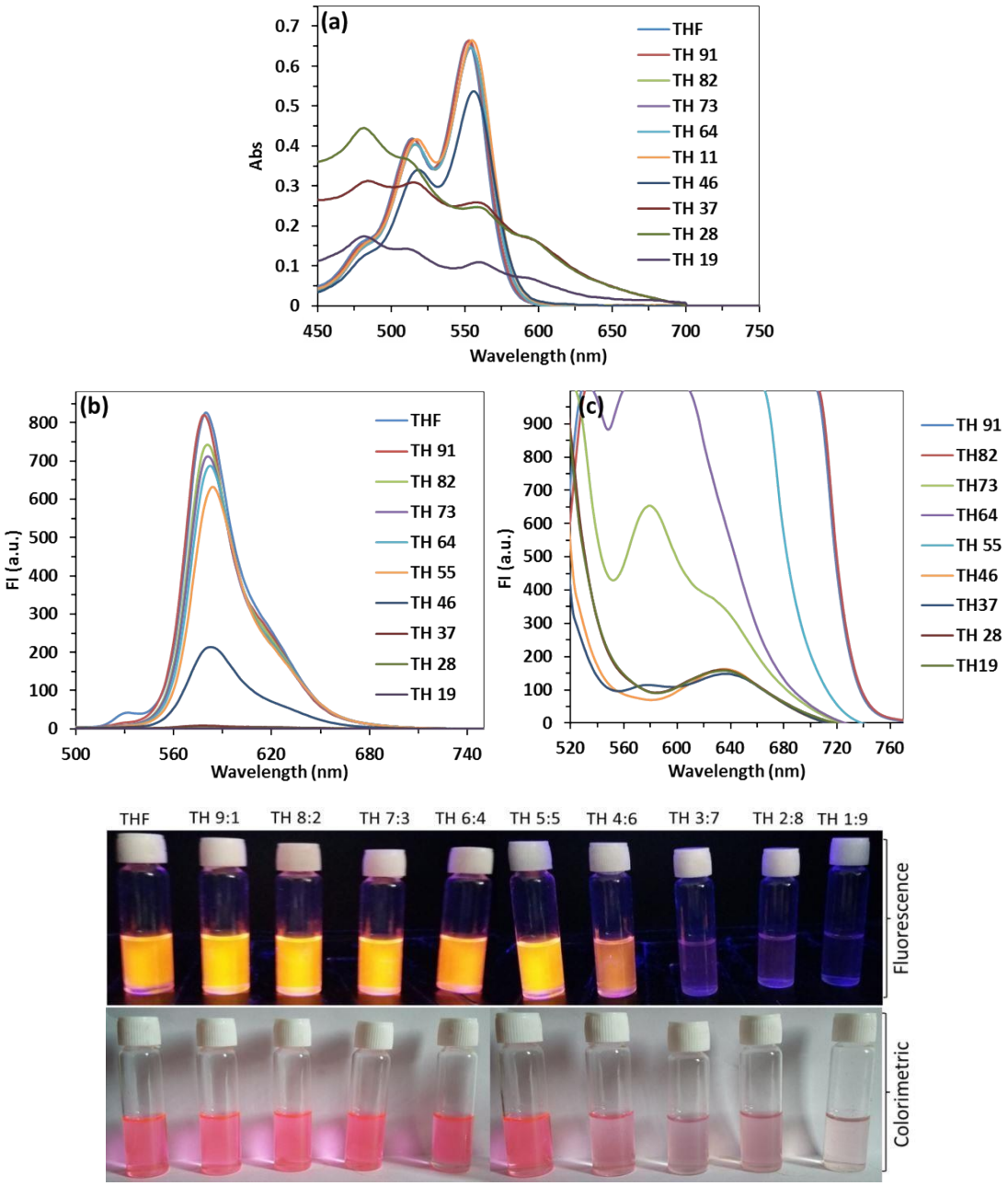

Fig. S7a. (Upper panel) (a) UV-Vis absorption spectra of **DPS-PDI** (10 μM) and (b) Fluorescence spectra of **DPS-PDI** (10 μM) after incremental addition of water in THF (λ_{ex} 470 nm, slit width Ex/Em = 15/3.5); (c) Fluorescence spectra of **DPS-PDI** (10 μM) after incremental addition of water in THF (λ_{ex} 490 nm, slit width Ex/Em = 20/20); (Lower panel) Fluorescence and Sunlight photographs of **DPS-PDI** (10 μM) after incremental addition of water in THF.

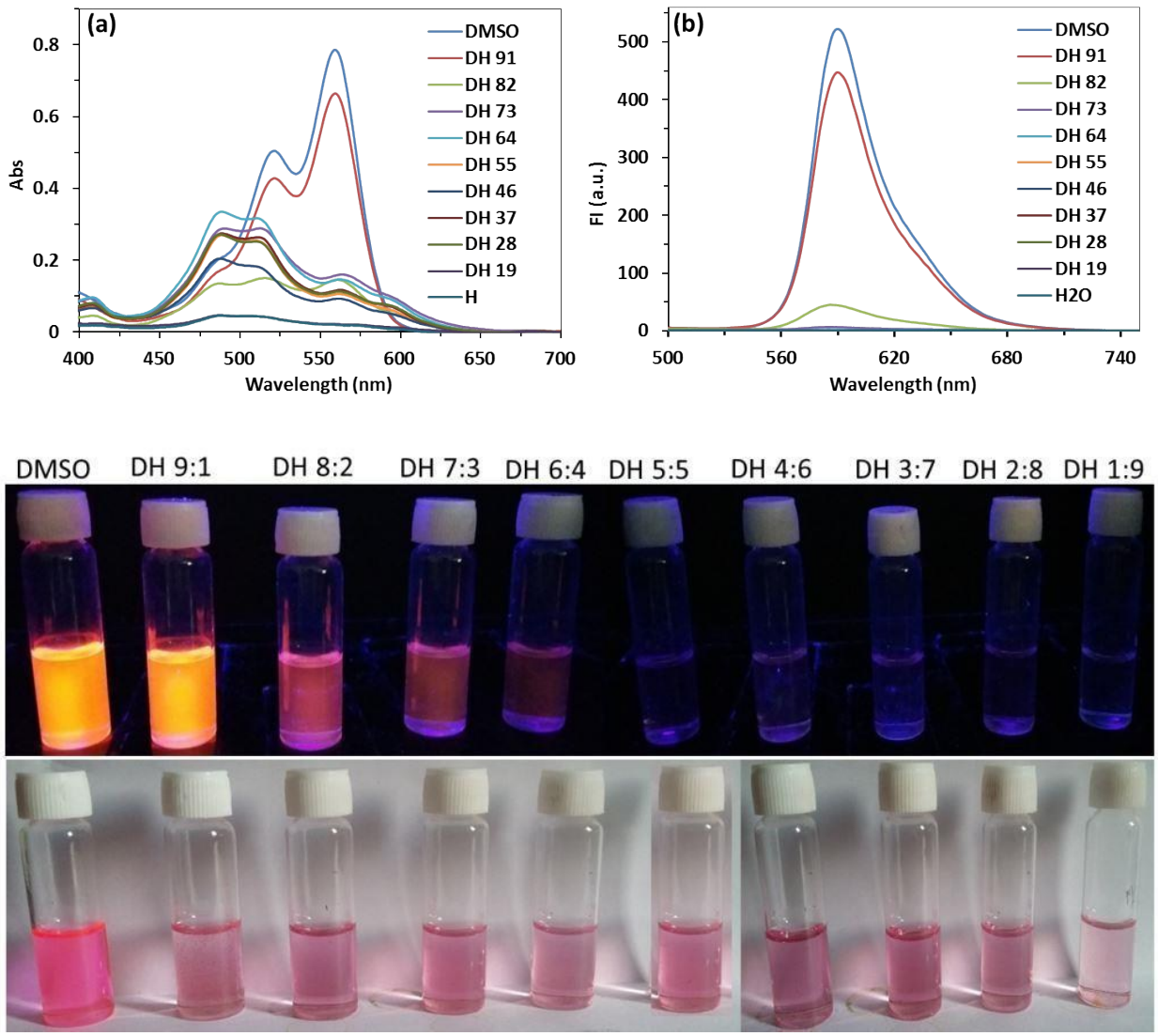

Fig. S7b. (Upper panel) (a) UV-Vis absorption spectra of **DPS-PDI** (10 μM) and (b) Fluorescence spectra of **DPS-PDI** (10 μM) after incremental addition of water in DMSO (λ_{ex} 470 nm, slit width Ex/Em = 15/3.5); (Lower panel) Fluorescence and Sunlight photographs of **DPS-PDI** (10 μM) after incremental addition of water in DMSO.

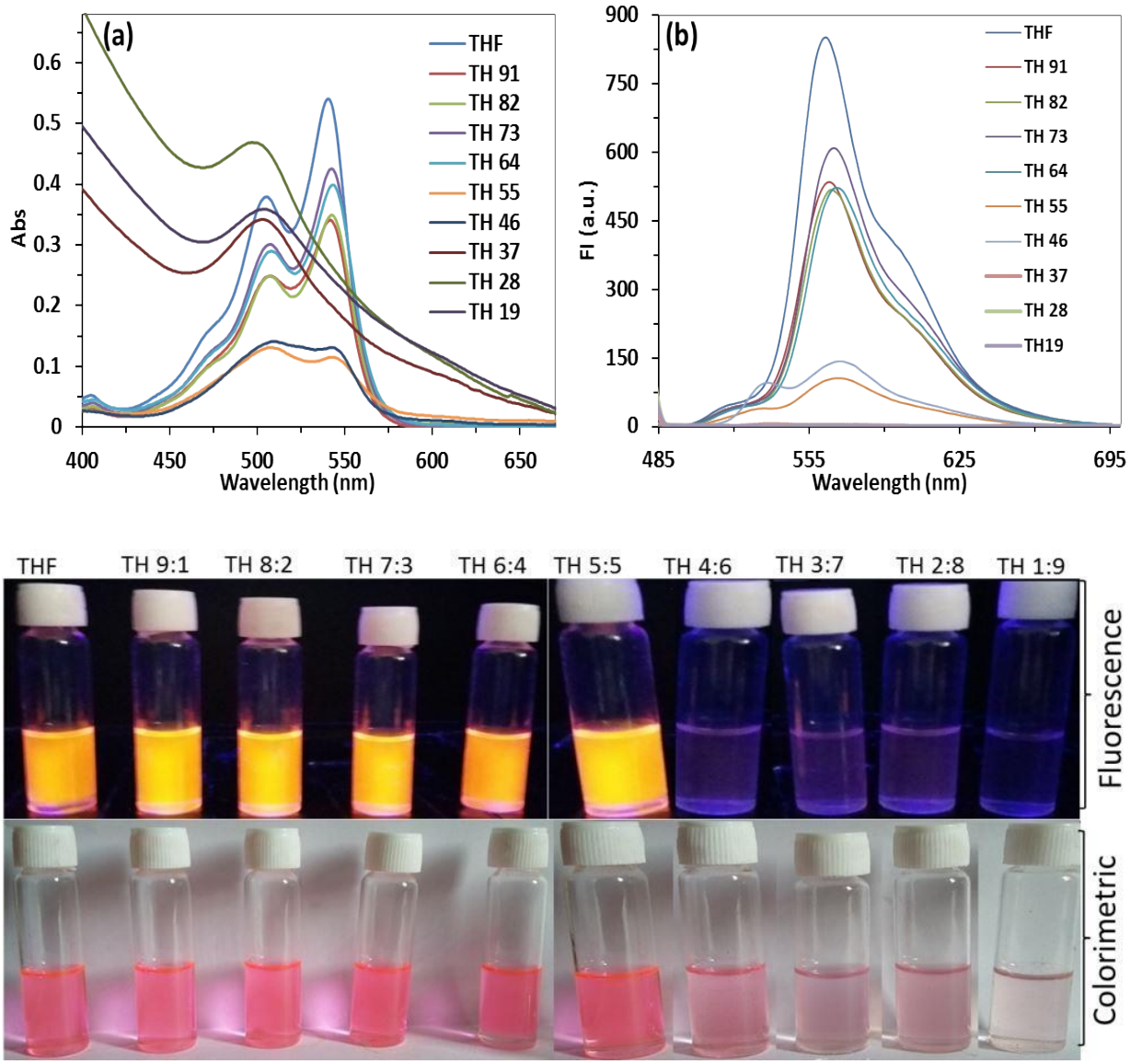

Fig. S8a. (Upper panel) (a) UV-Vis absorption spectra of PDI **5** (10 μM) and (b) Fluorescence spectra of PDI **5** (10 μM) after incremental addition of water in THF (λ_{ex} 470 nm, slit width Ex/Em = 14/2.8); (Lower panel) Fluorescence and Sunlight photographs of PDI **5** (10 μM) after incremental addition of water in THF.

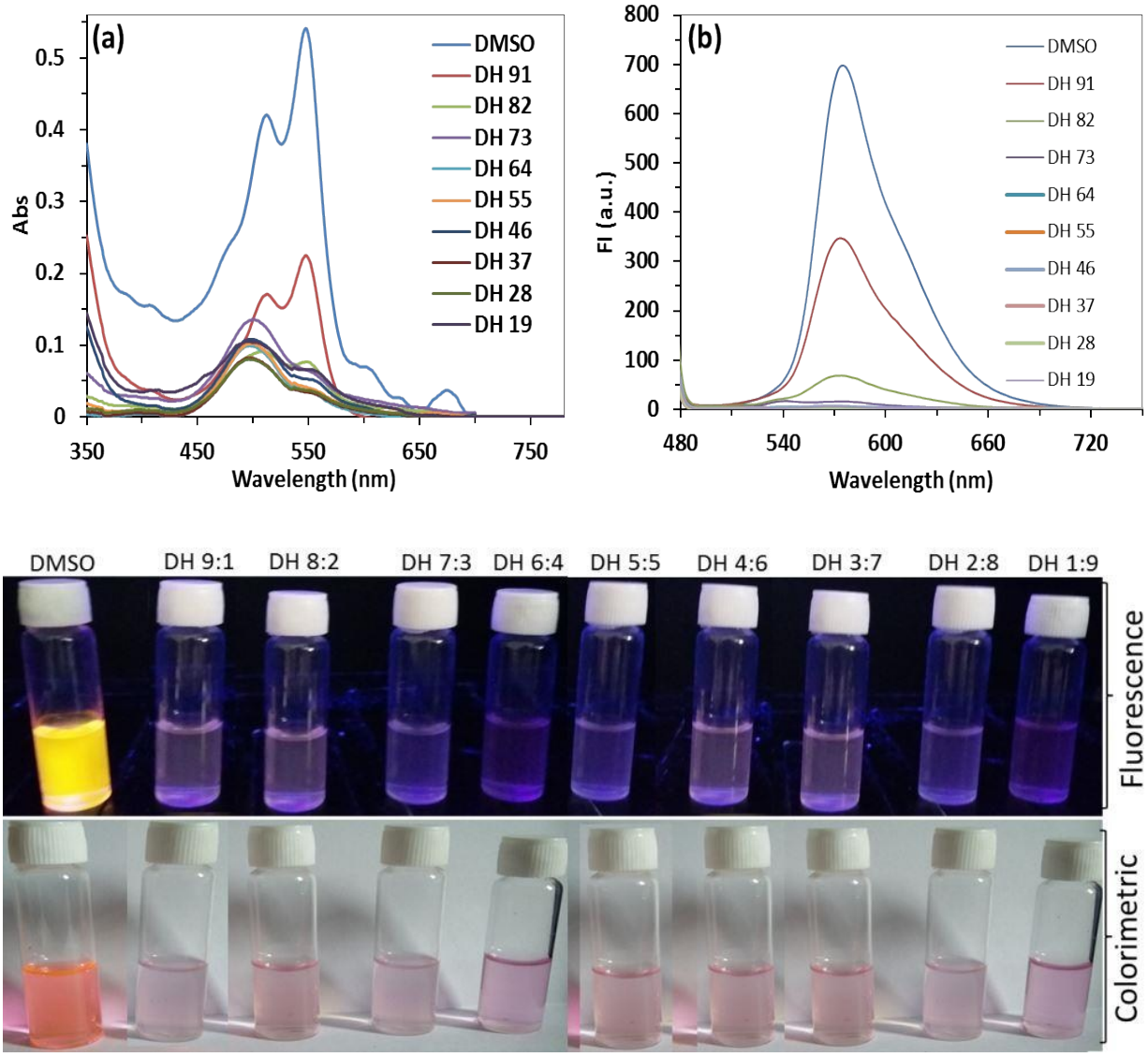

Fig. S8b. (Upper panel) (a) UV-Vis absorption spectra of PDI **5** (10 μM) and (b) Fluorescence spectra of PDI **5** (10 μM) after incremental addition of water in DMSO (λ_{ex} 470 nm, slit width Ex/Em = 14/3.5); (Lower panel) Fluorescence and Sunlight photographs of PDI **5** (10 μM) after incremental addition of water in DMSO.

4. PH titration of PS-PDI

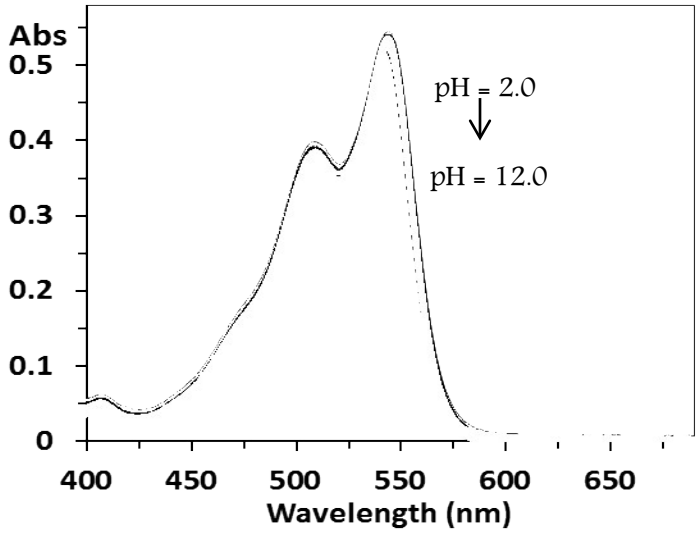

Fig. S9. The effect of PH on the absorption spectrum of **PS-PDI** (10 μM) recorded in THF:H_2O (1:1, v/v).

5. Self-assembly of PS-PDI in different solvents

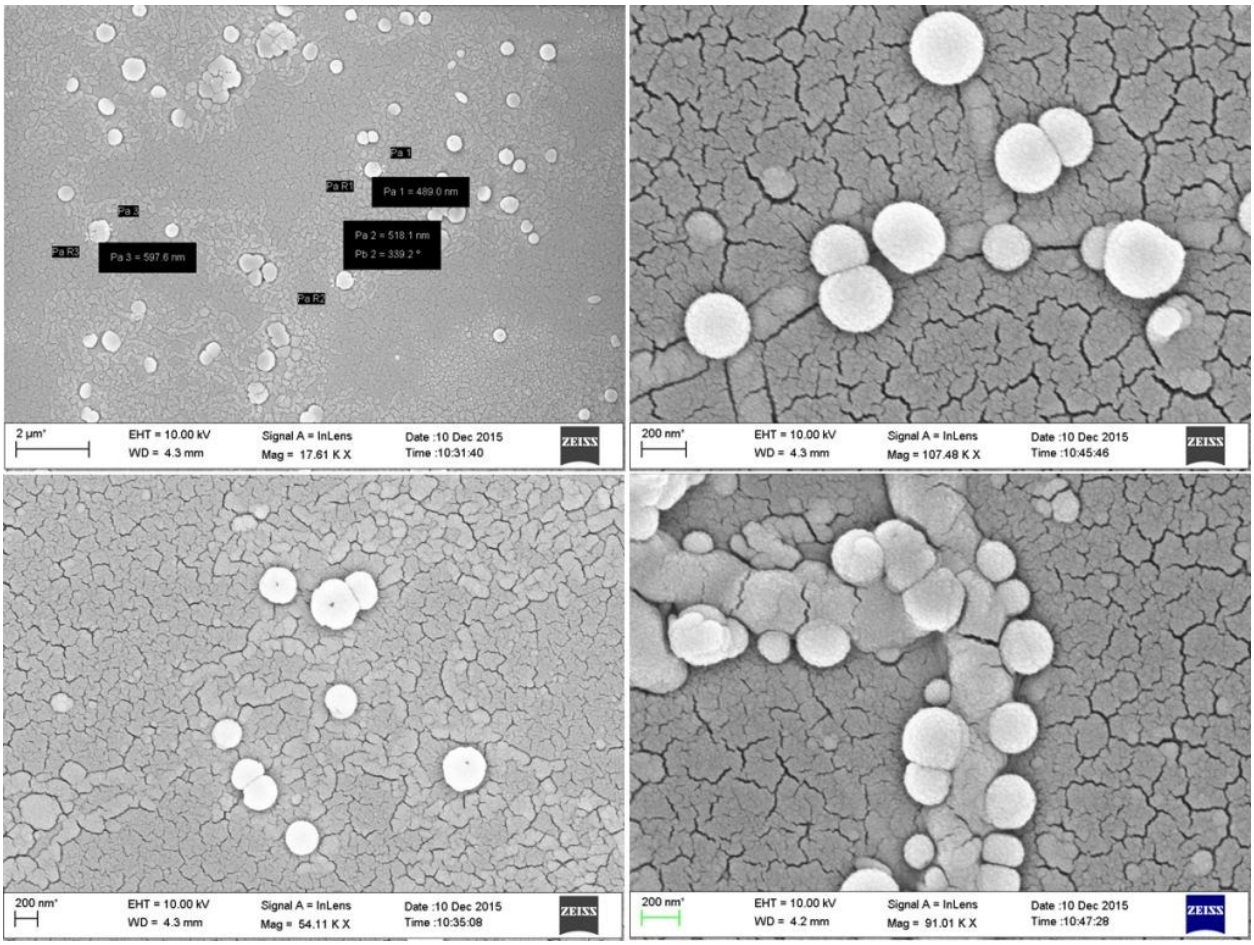

Fig. S10a. Nanospheres self-assembly of **PS-PDI** (10 µM) showing the presence of open hole on the surface of nanospheres. SEM images taken in H_2O:THF (1:1) solution.

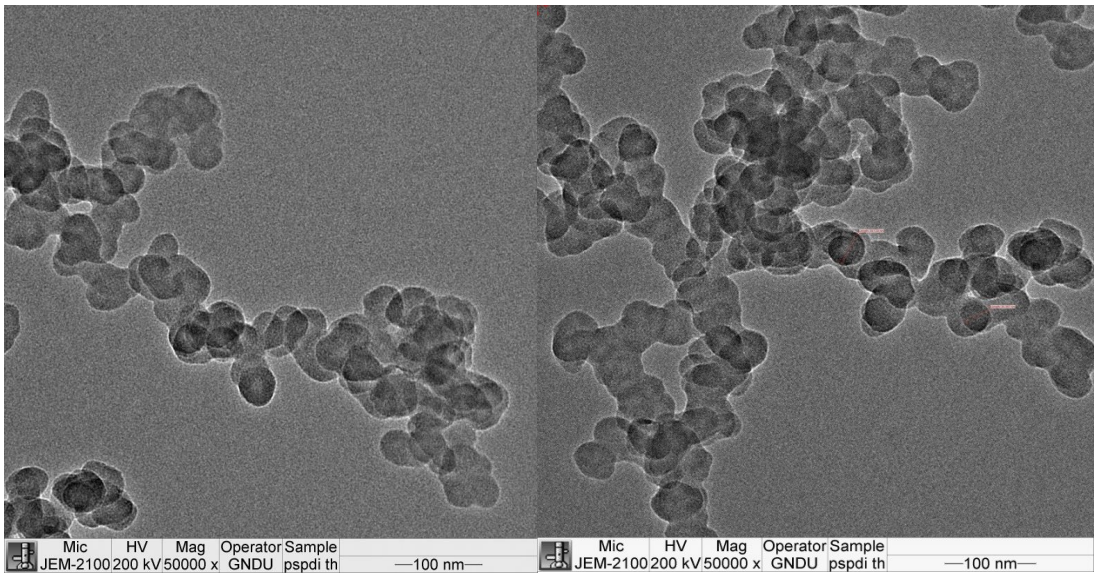

Fig. S10b. Nanospheres self-assembly of **PS-PDI** (10 μM). TEM images taken in H_2O:THF (1:1) solution.

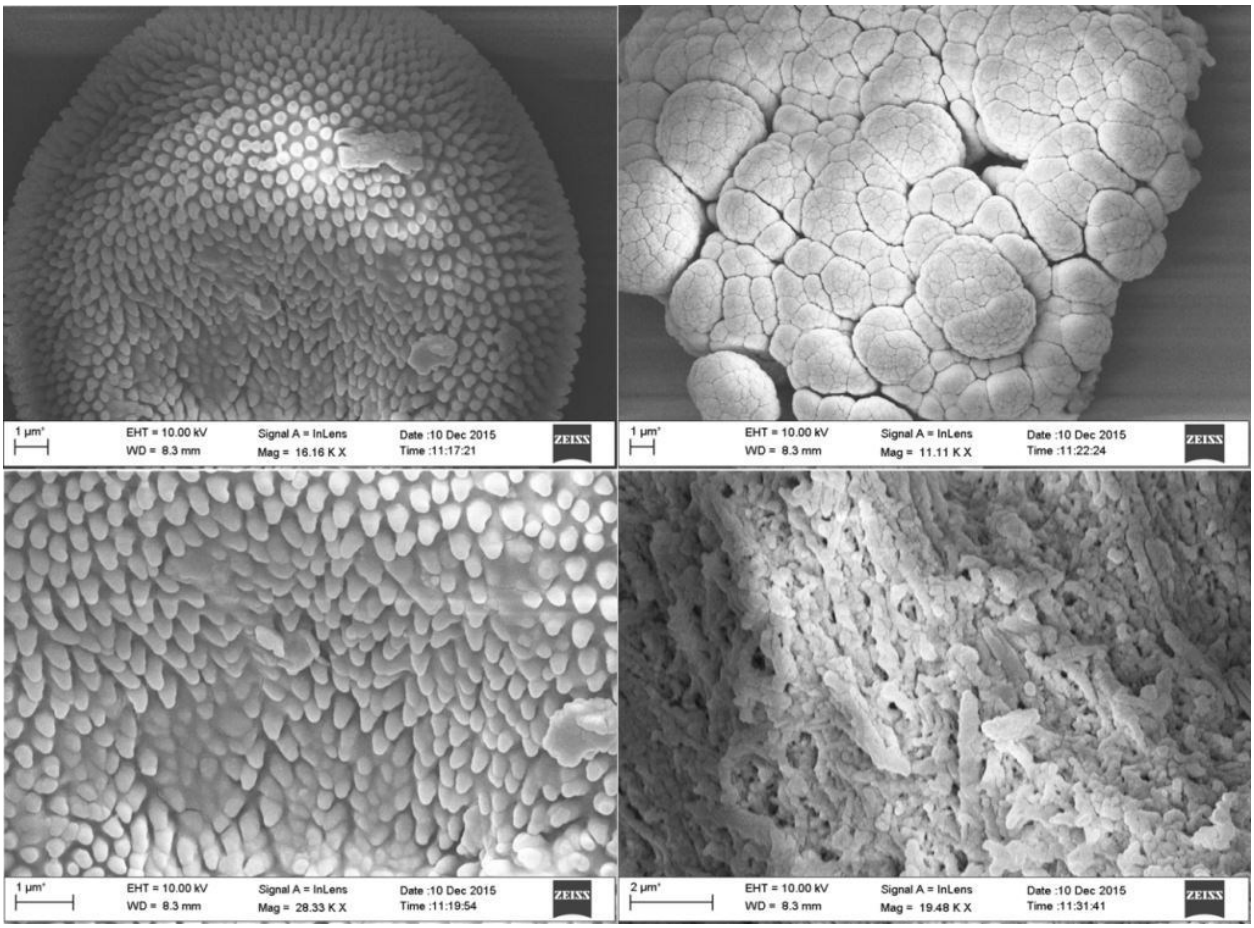

Fig. S11a. Nanorods and nano spheres self-assembly of **PS-PDI** (10 μM). SEM images taken in DMSO:H_2O (1:9) solution.

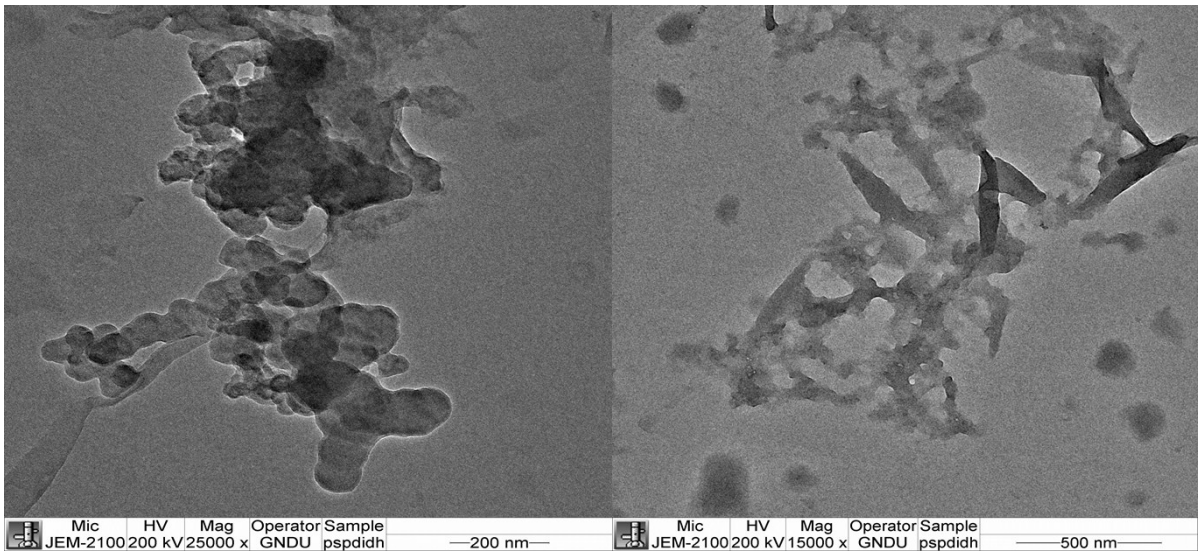

Fig. S11b. Nanorods and nano spheres self-assembly of **PS-PDI** (10 μM). TEM images taken in DMSO:H_2O (1:9) solution.

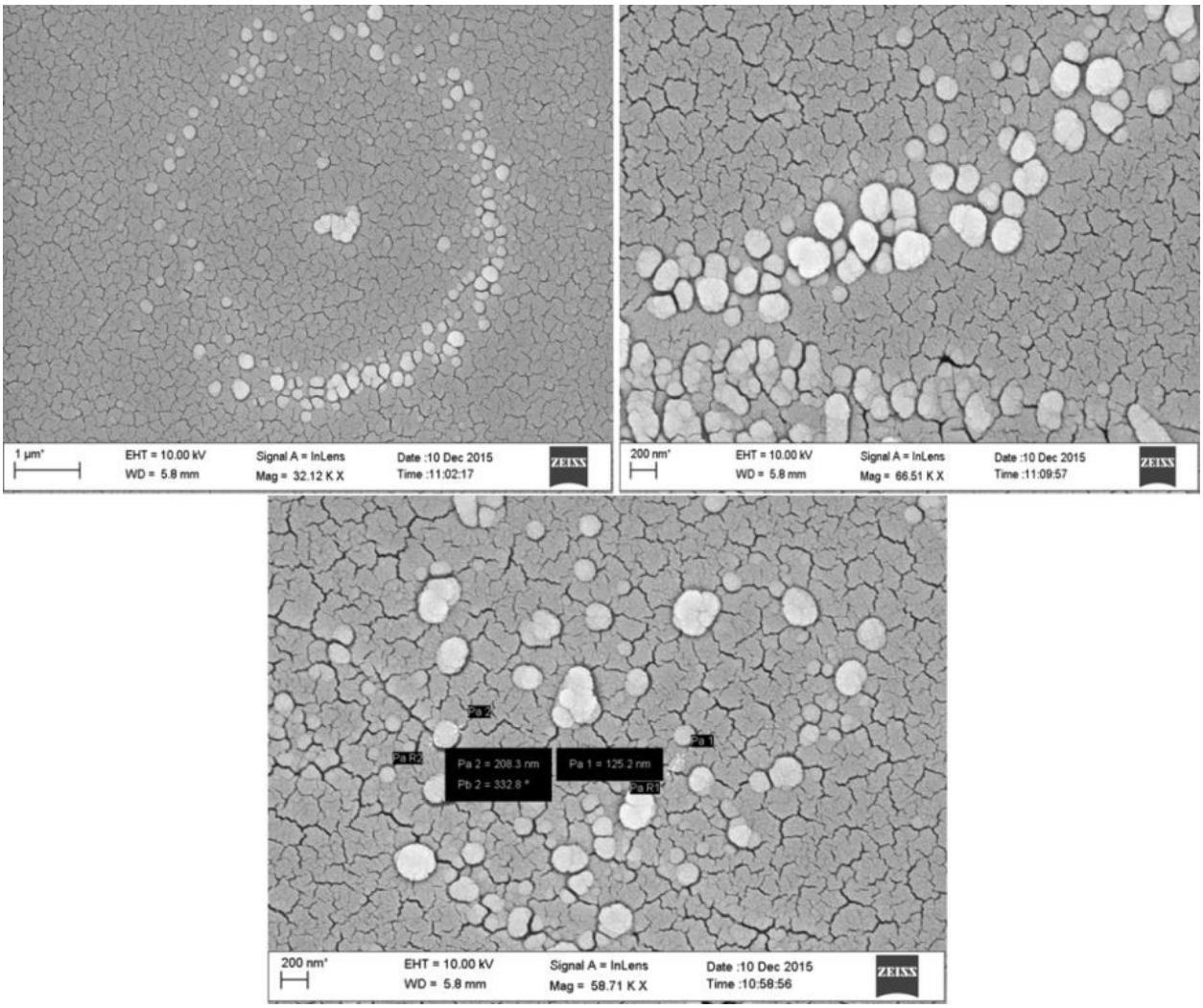

Fig. S12a. Nanospheres self-assembly of **PS-PDI** (10 µM) on addition of Pd^0 (100 µM). SEM images taken in THF:H_2O (1:1) solution.

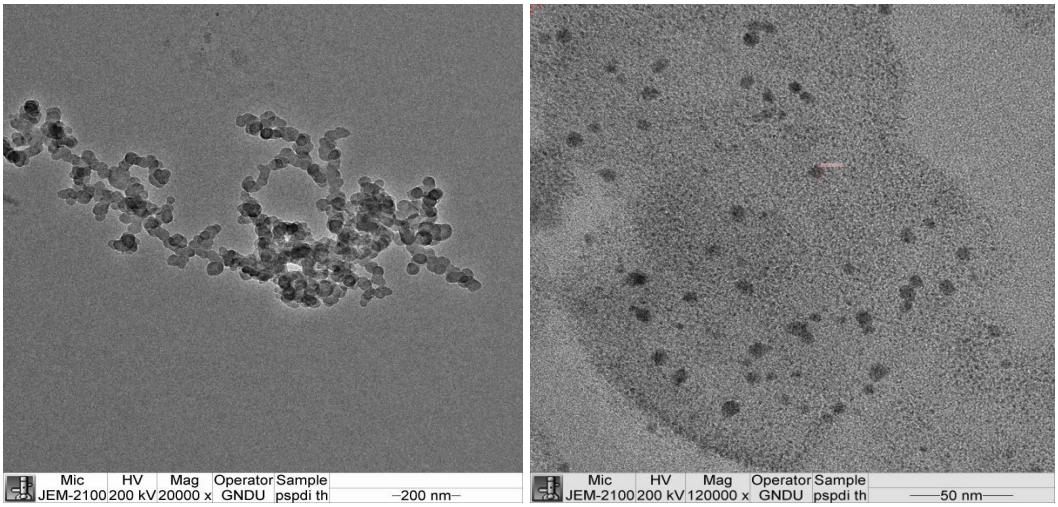

Fig. S12b. Nanospheres self-assembly of **PS-PDI** (10 µM) on addition of Pd^0 (100 µM). TEM images taken in THF:H_2O (1:1) solution.

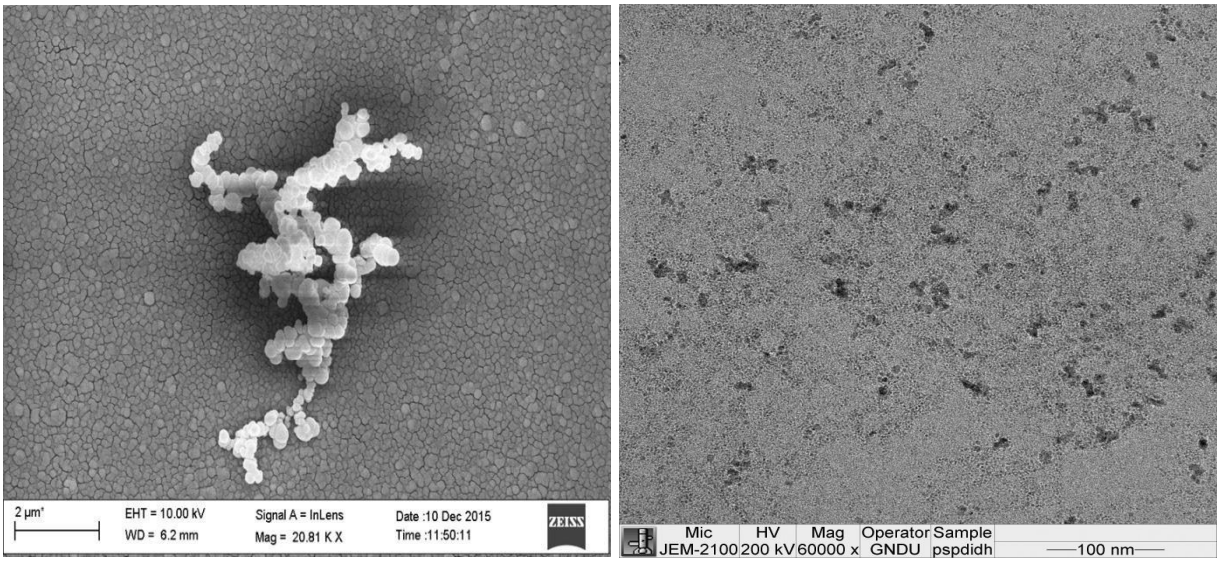

Fig. S13. Nanospheres self-assembly of **PS-PDI** (10 µM) on addition of Pd^0 (100 µM). SEM and TEM images taken in DMSO:H_2O (1:9) solution.

6. Photophysical properties of PS-PDI in DMSO:H_2O (1:9)

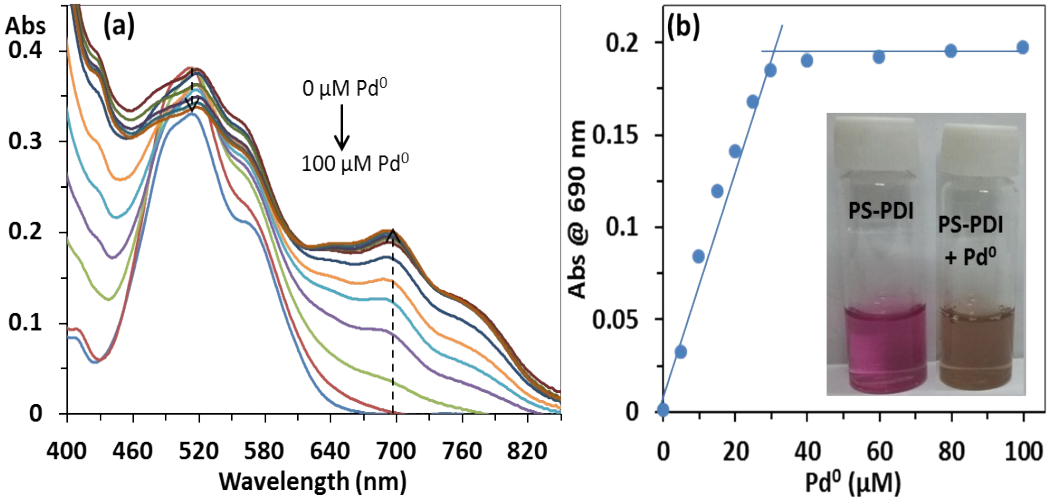

Fig. S14. (a) UV-Vis absorption spectra of **PS-PDI** (10 μM) after incremental addition of Pd^0 recorded in HEPES buffer-DMSO (9:1, v/v, pH 7.3); (b) Plot of absorbance intensity *vs* conc. of Pd^0 at 690 nm; Inset (b): naked eye colour change of **PS-PDI** (10 μM) on addition of Pd^0.

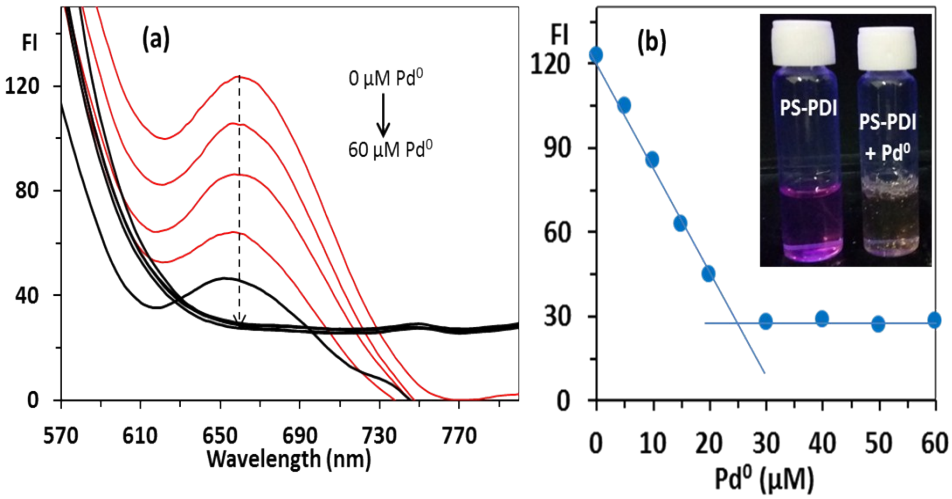

Fig. S15. (a) Fluorescence spectra of **PS-PDI** (10 μM) after incremental addition of Pd^0 recorded in HEPES buffer-DMSO (9:1, v/v, pH 7.3); (b) Plot of fluorescence intensity *vs* conc. of Pd^0 at 660 nm; Inset (b): fluorescent images of **PS-PDI** (10 μM) before and after addition of Pd^0 under illumination of UV light (365 nm).

6. Photophysical properties of DPS-PDI

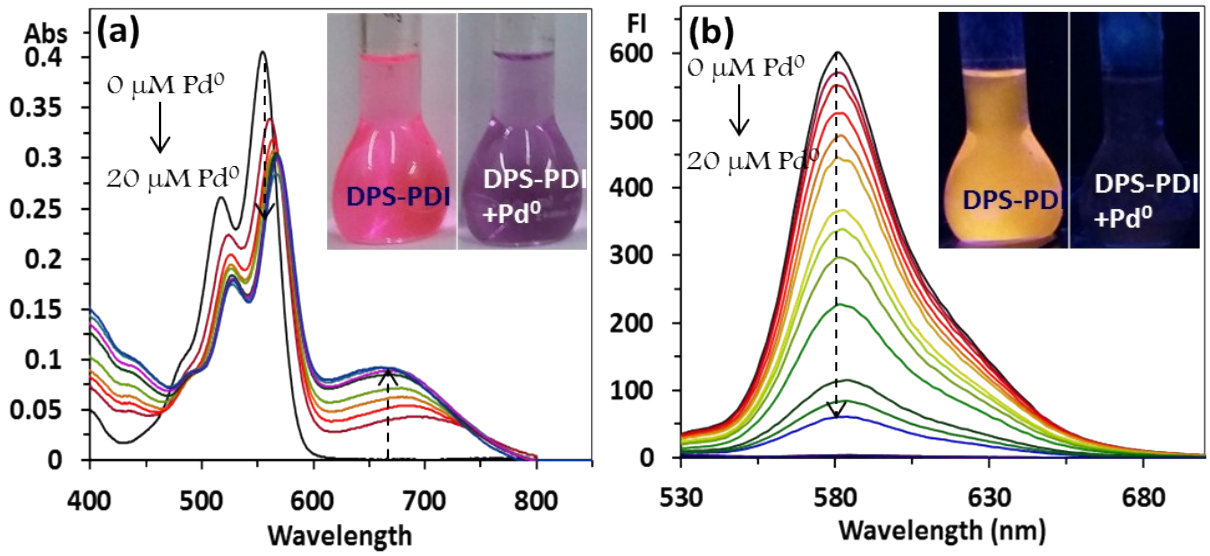

Fig S16. (a) UV-Vis absorption and (b) Fluorescence spectra of **DPS-PDI** (10 μM) after incremental addition of Pd0 recorded in HEPES buffer-THF (1:1, v/v, pH 7.3); All spectra were recorded after time interval of 1 hour.

8. MTT Assay

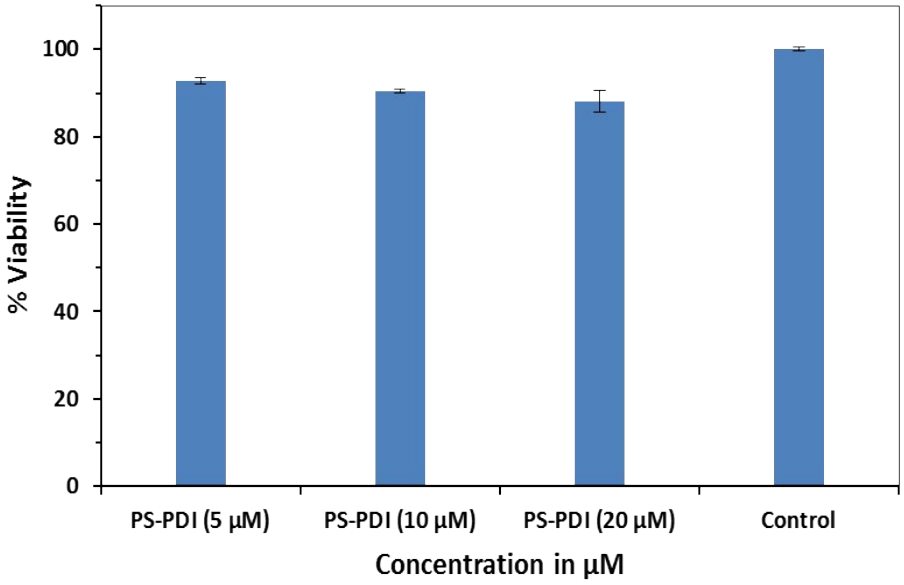

Fig. S17. Cell viability (%) tested by MTT assay using HeLa cells at 37 °C.

9. Time and concentration dependent Kinetic Profile

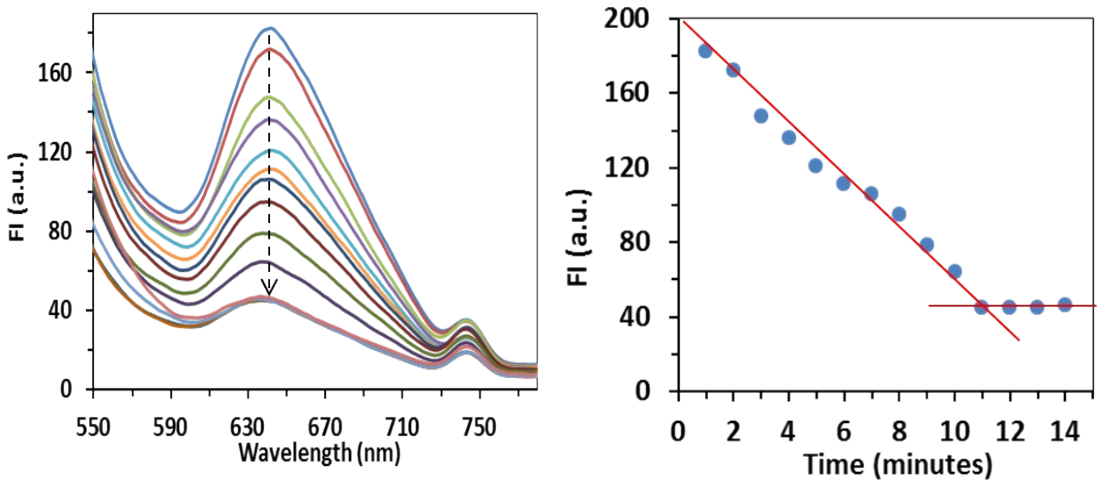

Fig. S18a. Time dependent kinetic profile for **PS-PDI** (10 µM) on addition of Pd^0 (5 µM) recorded in HEPES buffer-DMSO (9:1, v/v, pH 7.3); (Left) Emission changes of **PS-PDI** with regular time interval (Right) Plot of fluorescence intensity at 564 nm vs change in time.

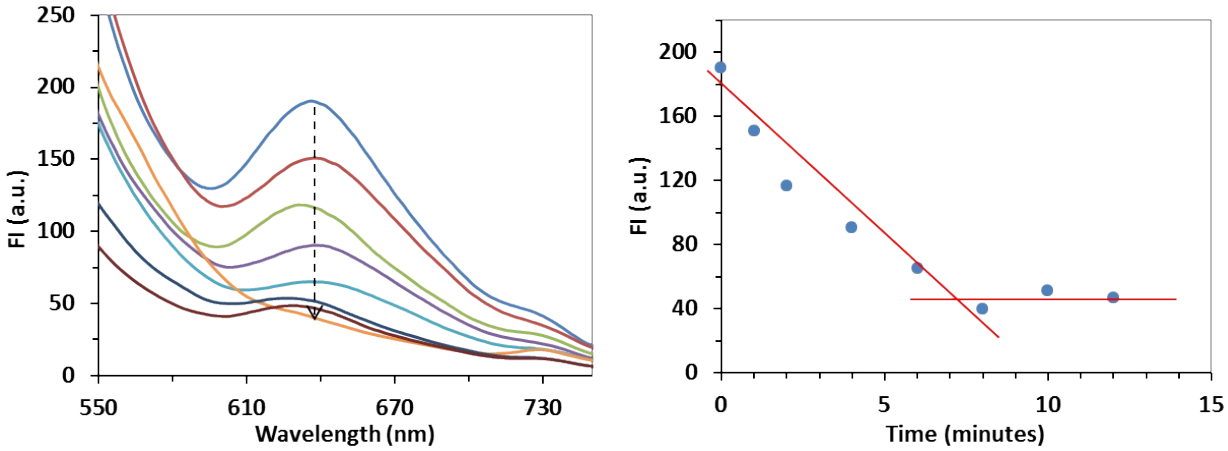

Fig. S18b. Time dependent kinetic profile for **PS-PDI** (10 µM) on addition of Pd^0 (10 µM) recorded in HEPES buffer-DMSO (9:1, v/v, pH 7.3); (Left) Emission changes of **PS-PDI** with regular time interval (Right) Plot of fluorescence intensity at 564 nm vs change in time.

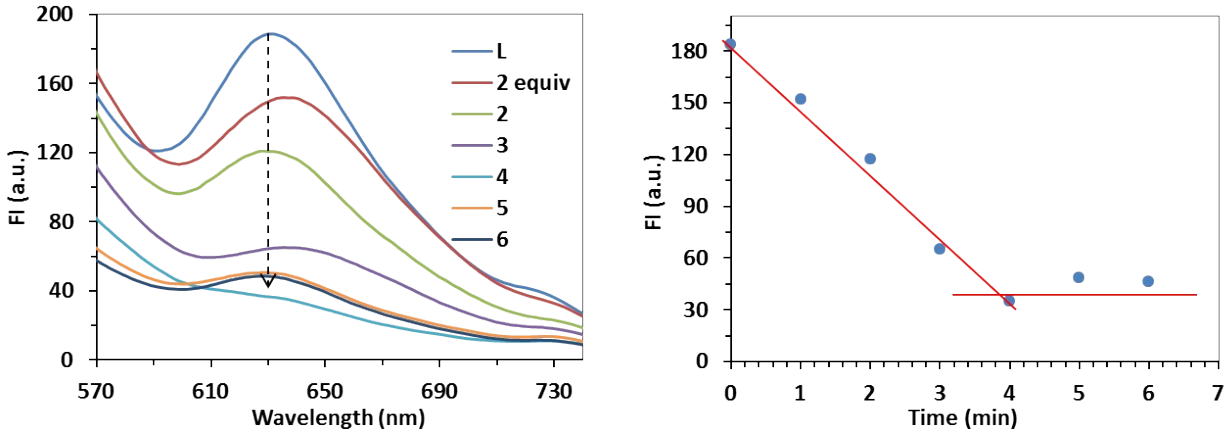

Fig. S18c. Time dependent kinetic profile for **PS-PDI** (10 μM) on addition of Pd^0 (20 μM) recorded in HEPES buffer-DMSO (9:1, v/v, pH 7.3); (Left) Emission changes of **PS-PDI** with regular time interval (Right) Plot of fluorescence intensity at 564 nm vs change in time.

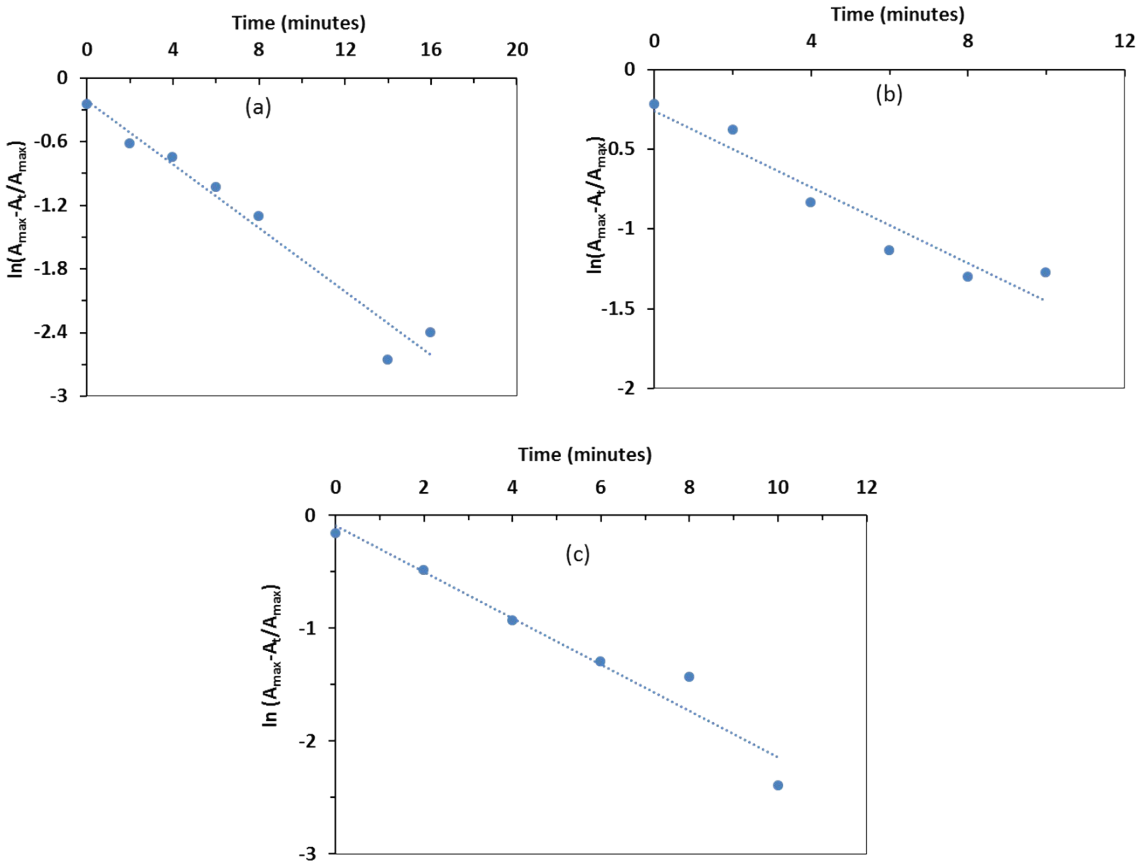

Fig. S19. Time dependent kinetic profile for **PS-PDI** (10 μM) on addition of Pd^0 (a) 5 μM (b) 10 μM and (c) 20 μM in HEPES buffer-DMSO (9:1, v/v, pH 7.3) by recording the absorption at 710 nm.

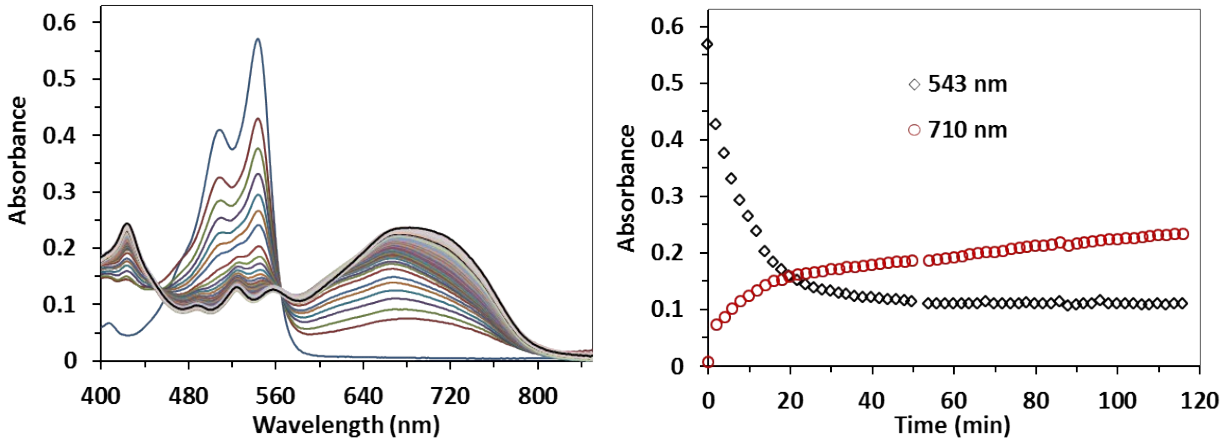

Fig. S20a: Time dependent kinetic profile for **PS-PDI** (10 µM) on addition of Pd^0 (60 µM) recorded in HEPES buffer-THF (1:1, v/v, pH 7.3); (Left) Absorbance changes of **PS-PDI** with regular time interval (Right) Plot of absorbance at 543 nm and 710 nm vs change in time.

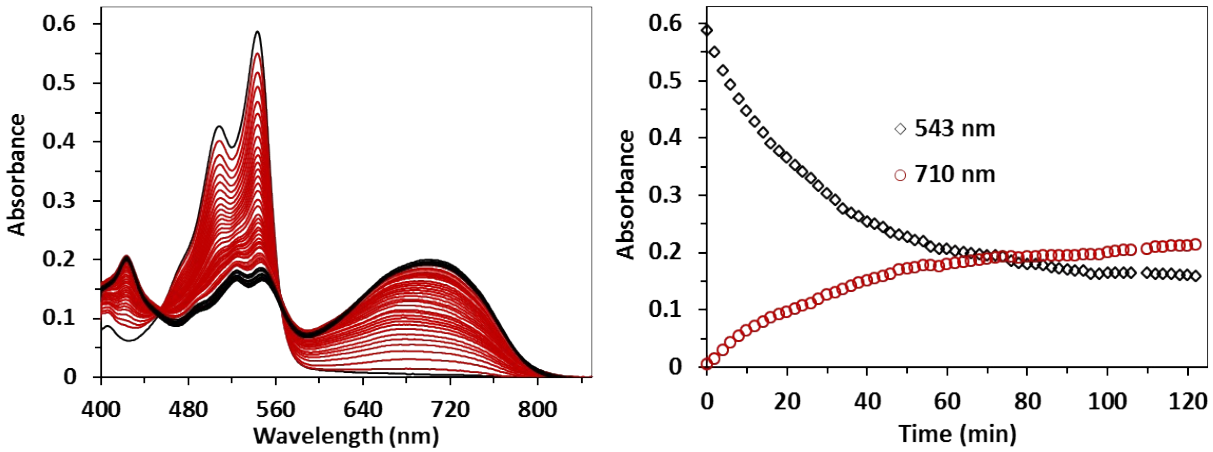

Fig. S20b. Time dependent kinetic profile for **PS-PDI** (10 µM) on addition of Pd^0 (40 µM) recorded in HEPES buffer-THF (1:1, v/v, pH 7.3); (Left) Absorbance changes of **PS-PDI** with regular time interval (Right) Plot of absorbance at 543 nm and 710 nm vs change in time.

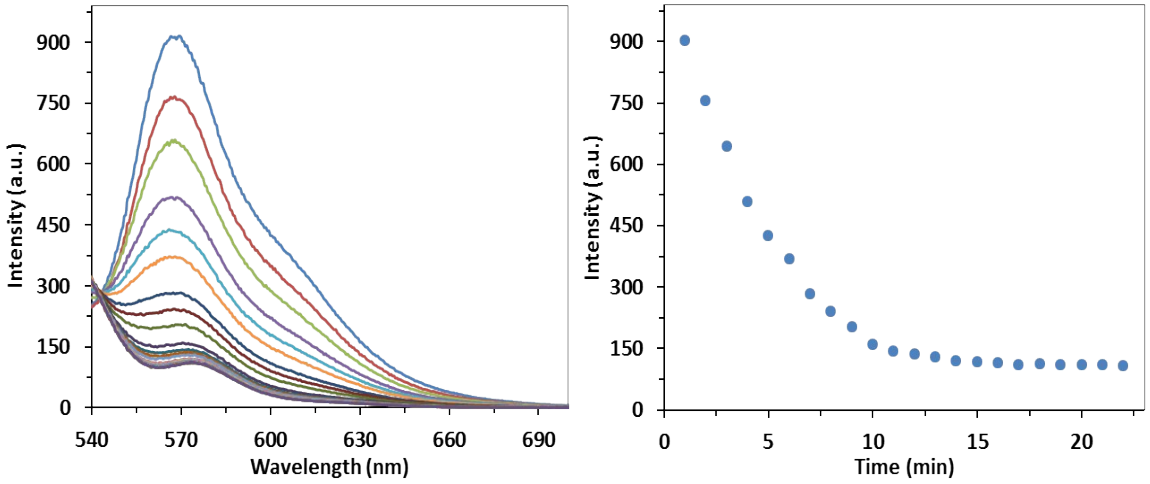

Fig. S21a: Time dependent kinetic profile for **PS-PDI** (10 µM) on addition of Pd^0 (60 µM) recorded in HEPES buffer-THF (1:1, v/v, pH 7.3); (Left) Emission changes of **PS-PDI** with regular time interval (Right) Plot of fluorescence intensity at 564 nm vs change in time.

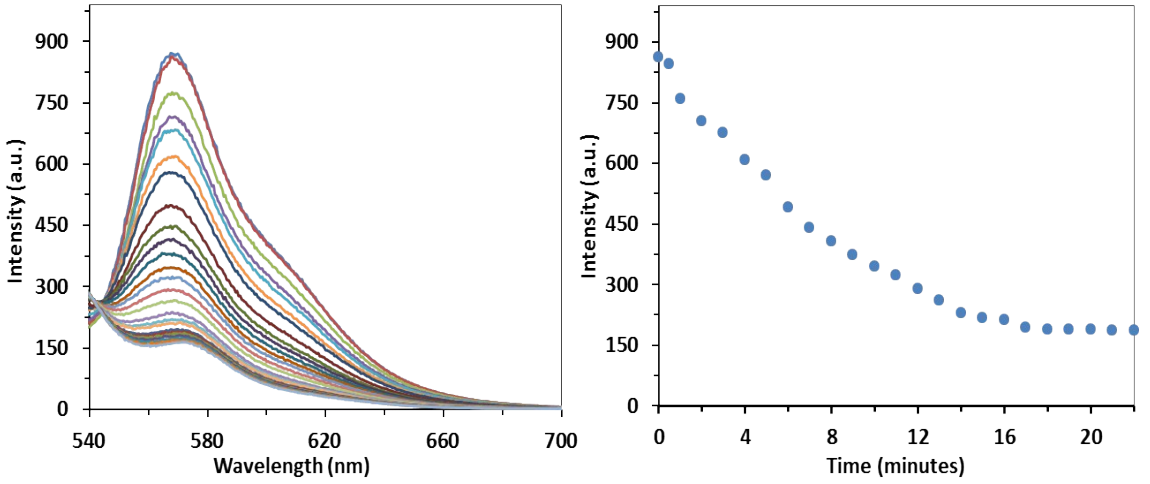

Fig. S21b. Time dependent kinetic profile for **PS-PDI** (10 µM) on addition of Pd^0 (40 µM) recorded in HEPES buffer-THF (1:1, v/v, pH 7.3); (Left) Emission changes of **PS-PDI** with regular time interval (Right) Plot of fluorescence intensity at 564 nm vs change in time.

10. Photophysical properties of PS-PDI with Pd^{2+}

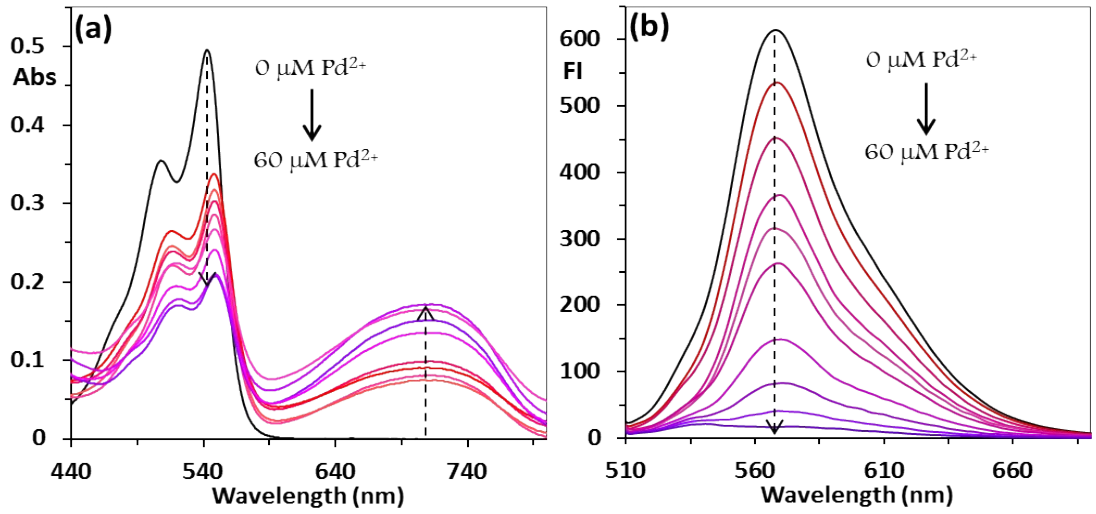

Fig S22 (a) UV-Vis absorption and (b) Fluorescence spectra of **PS-PDI** (10 μM) after incremental addition of Pd^{2+} recorded in HEPES buffer-THF (1:1, v/v, pH 7.3) in the presence of $NaBH_4$-PPh_3.

11. Analysis in the Environmental Samples

Table S2. Application of **PS-PDI** for determination of Pd^0 in the various environmental samples (tap water, pond water and industrial waste water).

(a) Tap water

UV-Vis Data (@710 nm)				**Fluorescence data@ 564 nm**			
Conc. (μM)	SD	% RSD	% Relative error	Conc. (μM)	SD	% RSD	% Relative error
5	0.076033	0.76033	1.075269	5	0.222726	2.227261	3.149823
10	0.186081	1.860807	1.315789	10	0.044297	0.442965	0.313224
15	0.58385	5.838496	2.752294	15	0.054855	0.548546	0.258587
20	0.563432	5.634317	1.992032	20	0.194435	1.944345	0.68743
25	0.550706	5.507062	1.557632	25	0.82536	8.253601	2.334471
PRSD = 3.90; PRE = 1.90				**PRSD = 2.70; PRE = 1.35**			

(b) Pond water

UV-Vis Data (@ 710 nm)				**Fluorescence data @ 564 nm**			
Conc. (μM)	SD	% RSD	% Relative error	Conc. (μM)	SD	% RSD	% Relative error
5	0.188266	1.882664	2.898551	5	0.013502	0.135018	0.186414
10	0.237267	2.372672	1.826484	10	0.503988	5.039877	3.739656
15	0.119048	1.190476	0.529101	15	0.270343	2.703426	1.378303
20	0.150286	1.502864	0.578453	20	1.342097	13.42097	5.159861
25	0.234763	2.347631	0.68306	25	0.33181	3.318105	1.021711
30	0.304569	3.045685	0.676819	30	0.898544	8.985443	2.178649
PRSD = 2.05; PRE = 1.2				**PRSD = 2.60; PRE = 2.30**			

(c) Industrial Waste Water

UV-Vis Data (@ 710 nm)				**Fluorescence data @ 710 nm**			
Conc. (μM)	SD	% RSD	% Relative error	Conc. (μM)	SD	% RSD	% Relative error
5	0.115919	1.159191	1.639344	5	0.046828	0.468283	0.662252
10	0.109629	1.09629	0.775194	10	0.811212	8.112124	3.824092
15	0.471405	4.714045	2.222222	15	0.107002	1.070023	0.37831
20	0.813936	8.139359	2.877698	20	0.058246	0.58246	0.164745
25	0.768594	7.685943	2.173913	25	0.084013	0.840127	0.19802
30	0.335829	3.358291	0.791557	30	0	0	0
PRSD = 4.35; PRE = 1.74				**PRSD = 1.84; PRE = 0.91**			

12. pH titration of PDI-OH

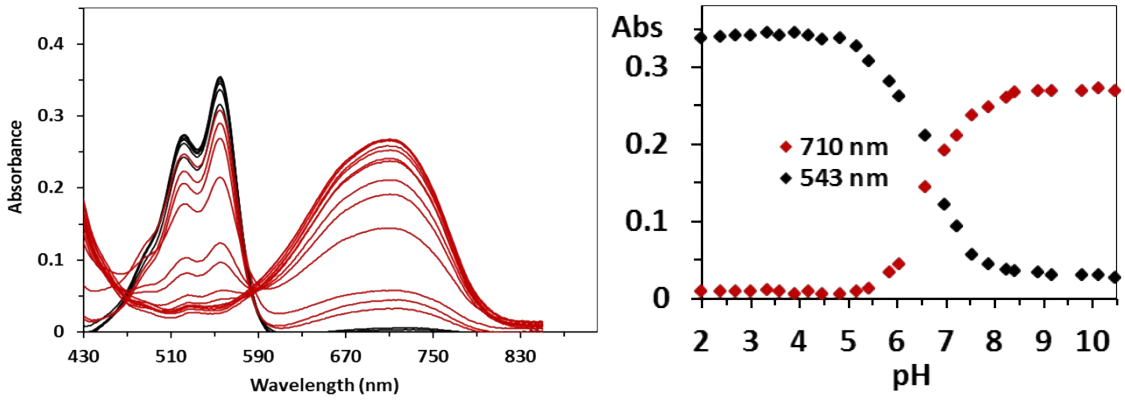

Fig S23. (Left) Effect of pH changes on the UV-Vis absorption spectrum of **PDI-OH** (10 μM) in water (50% THF); (Right) Plot of absorbance at 543 nm and 710 nm vs. change in pH of the solution.

13. Competition Experiments

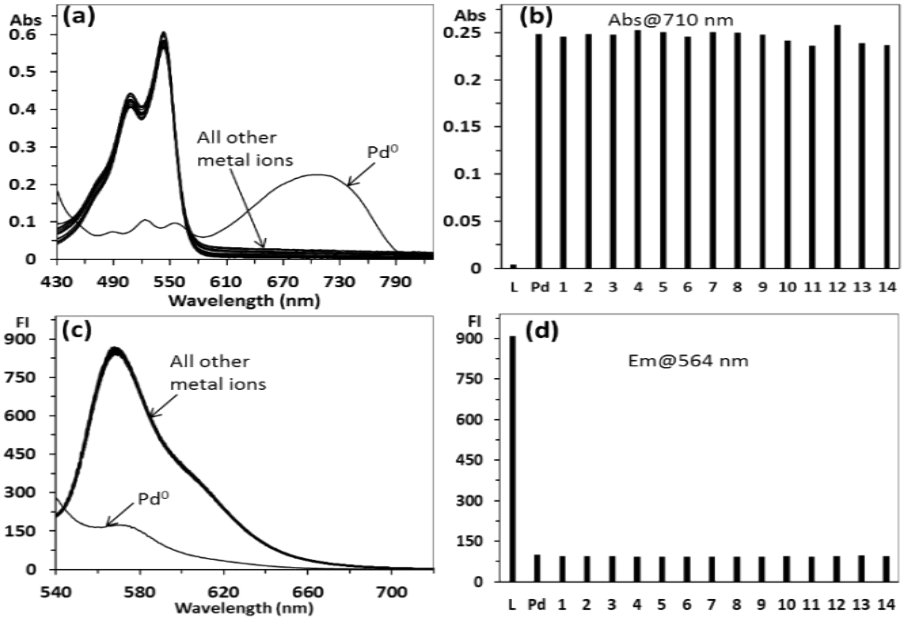

Fig. S24. (a) UV-Vis absorption (c) emission spectrum of **PS-PDI** showing the effect of various metal ions (100 μM); Bar diagram showing the effect of other metal ions (100 μM) on the **PS-PDI**+Pd^0 mixture in the (b) absorption and (d) emission spectrum; **1** = L+Pd^0+Zn^{2+}; **2** = L+Pd^0+Ni^{2+}; **3** = L+Pd^0+Hg^{2+}; **4** = L + Pd^0 + Li^+; **5** = L + Pd^0 + K^+; **6** = L +Pd^0 + Cs^+; **7** = L + Pd^0 + Ba^{2+}; **8** = L + Pd^0 + Co^{2+}; **9** = L + Pd^0 + Ca^{2+}; **10** = L + Pd^0 + Mg^{2+}; **11** = L + Pd^0 + Pb^{2+}; **12** = L + Pd^0 + Sr^{2+}; **13** = L + Pd^0 + Fe^{2+}; **14** = L + Pd^0 + Cu^{2+}.